J. Fluid Mech. (1991), *vol.* 229, *pp.* 311–338
Printed in Great Britain

A general theory of curved vortices with circular cross-section and variable core area

By J. S. MARSHALL
Department of Ocean Engineering, Florida Atlantic University, Boca Raton, FL 33431, USA

(Received 29 May 1990 and in revised form 17 January 1991)

A theory is derived for general motions of an inviscid vortex with circular cross-section and variable core area using a directed filament model of the vortex. The theory reduces in special cases to any of several previous vortex theories in the literature, but it is better suited than previous theories for handling nonlinear area-varying waves on the vortex core. Jump conditions across points of discontinuity and a variational form of the theory are also given. The theory is applied to obtain new solutions for several fundamental problems in vortex dynamics related to axisymmetric solitary waves on a vortex core, axisymmetric and helical vortex breakdowns and the buckling of a columnar vortex under compression.

1. Introduction

A theory is presented in this paper for arbitrary motions of inviscid vortices under the simplifying constraint that the vortex cross-section remain circular. Extension of the theory to treat vortices with elliptical cross-sections is fairly straightforward, although for brevity it is not pursued in the present paper. The theory is used to obtain new results for nonlinear area-varying waves on vortex cores, axisymmetric and helical vortex breakdowns and a phenomenon referred to here as 'vortex buckling'.

The literature on vortex dynamics is extensive and spans a considerable time period, but only a few studies have turned from the solution of particular problems to consider a general theory of vortex motion. One notable early attempt at a general theory is that of Betchov (1965), who considered the motion of curved vortices with constant core area and no axial flow. Betchov derived equations for the curvature and torsion of a vortex filament by assuming that every point of the filament is convected with the velocity induced from the circulation of neighbouring points on the filament. A milestone in vortex dynamics was reached with the papers of Widnall & Bliss (1971) and Moore & Saffman (1972), hereinafter referred to respectively as WB and MS, who developed theories of vortex filaments containing axial flow. Both of these latter studies recognized that the velocity of a vortex may differ from the so-called 'induced' velocity, and in order to predict vortex motion the 'external forces' acting on the lateral core surface must be balanced against the 'internal forces' of the vortex. This analysis was recently extended by Lundgren & Ashurst (1989), hereinafter referred to as LA, to study propagation and evolution of waves of varying vortex core area (i.e. axisymmetric waves). The theory proposed by LA is analogous in many respects to the long-wave theory used for surface waves in shallow waters. In particular, the theory assumes that the radial centrifugal pressure gradient set up by steady motion of the vortex is undisturbed by the wave motion (which is similar

to the hydrostatic pressure assumption used in nonlinear shallow-water wave theory). This assumption neglects the effects of radial inertia, which may be substantial in the light of typical experimental descriptions of axisymmetric vortex waves (e.g. Maxworthy, Hopfinger & Redekopp 1985) as quite nonlinear and propagating extremely fast. Nevertheless, the approach taken in LA, especially with regard to the treatment of vortex breakdown, has been instrumental to the present study, and it is reasonable to expect that the results of LA should be valid in certain limits.

The vortex theory in the present paper is motivated by the nonlinear water wave theory of Green & Naghdi (1976), in which a three-dimensional fluid layer is modelled by a 'directed fluid sheet' (a surface-like structure containing additional vector variables, called directors, that typically point along the normal to the surface or in some other direction not tangent to the surface). The Green–Naghdi wave theory can also be formulated as a variational statement of Hamiltonian form and is found to reduce to the standard Korteweg–de Vries and Boussinesq nonlinear wave theories as special cases (Miles & Salmon 1985).

To be more specific, a vortex is assumed in this paper to consist of a core which at each infinitesimal section along its length is exposed to an external flow composed of a potential vortex, a source or sink coincident to the vortex and a uniform flow (not necessarily directed normal to the vortex axis). The uniform external flow may consist of an 'induced' velocity (caused by neighbouring sections of the filament when the vortex is curved) and some other prescribed flow field, which is restricted only in that the typical lengthscale L of the prescribed flow be much greater than the core radius σ. It is assumed that the axial velocity is uniform across the core and that the core rotates as a solid body. This assumption, which is made for simplicity, presumes that the effect of the internal core dynamics on the overall vortex motion can be expressed adequately through integral quantities and is not very sensitive to the precise form of the core velocity profile. Additionally, it is assumed that the product of vortex curvature κ and core radius σ is small compared to unity. To summarize, the four assumptions – $\kappa\sigma \ll 1, \sigma/L \ll 1$, uniform axial velocity and solid-body rotation in the core, and circular core cross-section – are all that are necessary for development of the present theory from the general equations of inviscid incompressible flow. These same assumptions are also made in the previously mentioned vortex theories proposed by LA, MS, WB and Betchov.

The vortex motion is determined by invoking a model of the vortex core as a 'directed filament', with two directors, which is subject to 'contact body forces' arising from forces exerted on the lateral core surface by the external flow. The general equations of motion for the vortex core are developed from the theory of Caulk & Naghdi (1979) for twisting jets together with an extended version of the external forces derived by MS. These equations include conservation of mass, a balance of 'ordinary' momentum, and a balance of 'director' momentum (for each director), as well as a constraint representing incompressibility of the fluid and another requiring the directors to be aligned normal to the vortex axis. As mentioned previously, the simplification of circular core cross-section is also made such that the two director momentum equations become identical.

The existing general theories of vortex motion form a type of hierarchy in that each theory reduces to earlier theories in limiting cases. The present theory reduces to that of LA as a special case and is hence no exception to this rule. However, not only is the manner of derivation of the theory quite different from that used in previous vortex theories, but the range of problems to which the theory applies is

considerably broader. By analogy, it is well known that the nonlinear shallow-water theory for free-surface waves has very limited range of applicability in comparison to the more general Boussinesq, Green–Naghdi, or Korteweg–de Vries theories, and in particular that the former theory does not admit a solution for solitary waves (see Wehausen & Laitone 1960, p. 702).

Following derivation of the general theory in §2, a number of applications of the theory are made in §§3–5 which illustrate some of the advantages of the present approach. Section 3 deals mainly with nonlinear axisymmetric waves on vortex cores and a solution for a stationary solitary wave is obtained which reduces in one limit to the sech^2 form suggested by Benjamin (1962). A brief preliminary discussion is also given in §3 on vortex rings and helical vortex waves. In §4, jump conditions across axisymmetric and helical vortex breakdowns are obtained, together with necessary conditions for the existence of breakdown of each type. A discussion is given in §5 on a phenomenon referred to here as vortex buckling which does not seem to have been previously discussed in the literature. The idea, which is very similar to the buckling of solid rods, is that a vortex will 'bend' when compressed axially if the amount of compression is greater than a critical amount, whose value depends upon the ratio of core radius to axial length. Using a Hamiltonian version of the theory derived in §2, this notion of vortex buckling is theoretically verified and the relationship of critical compression to the ratio of core radius divided by axial length is derived. Before leaving this section, it is noted that, for brevity, the discussion in §§3–5 focuses on new results obtained by use of the present theory and is not intended to provide an overview of previous work done on these problems.

2. Development of the general theory

This paper is concerned with a theory for vortices as distinct fluid entities. Accordingly, we introduce a *model* for the vortex which has the form of a one-dimensional continuum structure, which we refer to as a *directed vortex filament*, although it clearly has the form of a Cosserat curve used in other contexts (e.g. Green, Naghdi & Wenner 1974). A directed curve model has its own balance laws and its own constitutive equations for dependent variables appearing in these balance laws. The general balance laws (equations (2.8)–(2.11)) are the same for all directed curve theories, whether applied to vortex cores, fluid jets or elastic rods; only the constitutive equations, constraints on the independent variables, and body forces to which the directed curve is subject vary depending on the type of structure represented by the model. Typically, it is possible to rederive the equations of motion of the directed curve theory by an approximate procedure using the governing equations of the three-dimensional fluid continuum theory. Such an alternative derivation (a further description of which is given later in this section) is useful for motivating constitutive equations, constraints and body forces in the directed curve theory. Although the directed curve model may not be absolutely necessary for development of the equations of vortex motion given in this paper, use of the model offers three clear advantages: (i) It provides guidance and restrictions to development of approximate formulations from the three-dimensional theory. (ii) It provides a clear and concise kinematical structure for consideration of gross properties of the vortex, such as 'external forces' acting on the vortex and 'internal momentum' of the vortex. (iii) It provides a simple method of obtaining jump conditions across discontinuities which would otherwise be extremely difficult to derive.

The kinematics and equations of motion for the vortex filament can be obtained

as a special case of the theory of Caulk & Naghdi (1979) for an inviscid elliptical jet with twist after (i) invoking a constraint requiring the directors to be oriented orthogonally to the vortex axis and (ii) modifying the ordinary and director-assigned force fields for the free jet (resulting from gravity) to account for 'external' forces acting on the lateral surface of the vortex core. These external forces on the vortex are obtained by an extended version of the results obtained by MS.

To be more specific, the vortex is modelled in this paper by a material curve $\mathscr{R}$ to which, at every point of $\mathscr{R}$, we attach some number of vector-valued variables called directors. The curve $\mathscr{R}$ is chosen to be coincident with the centreline of the vortex core, and the directors are chosen to be orthogonal to each other and to the vortex centreline. The magnitude of the directors is identified with the core radius, and the rate of spin of the directors about the curve $\mathscr{R}$ is identified with the rotation rate of the vortex core times the core radius. Each material point on the directed vortex filament at every instant of time is assigned a position in space (the position of the vortex centreline), a velocity component parallel to $\mathscr{R}$ (the axial velocity in the core), velocity components normal to $\mathscr{R}$ (velocity of the vortex normal to the centreline), two directors (whose magnitudes give the vortex core radius) and the material derivatives of these directors (which can be used to find the rotation rate of the vortex core). The goal of the present theory is to derive reasonable and fairly general equations of motion for the vortex (giving the change with time of the aforementioned quantities characterizing the state of the vortex), which take into account effects due to internal forces and momentum and external forces acting on the core surface (which may be caused by self-induced velocity of the vortex, external prescribed flow past the vortex, or radial pressure gradient in the irrotational flow surrounding the core).

The balance laws for the directed vortex filament include equations for vortex mass density, 'ordinary' vortex momentum and 'director' momentum. The vortex mass density is the mass of fluid contained in the vortex core per unit axial length. Ordinary vortex momentum is the integrated momentum across the vortex per unit length and may be oriented either along the vortex axis or normal to the axis. Director momentum may have components in both the radial and circumferential directions, which can be identified, respectively, with the radial inertia incurred during a change in core radius and with the product of the vortex mass, the core rotation rate and the core radius.

2.1. *Kinematics and balance laws for the vortex filament*

The material directed curve $\mathscr{R}$ occupies a space curve $\mathscr{C}$ in Euclidian 3-space at time t, such that the position of a point X on $\mathscr{C}$, relative to a fixed Cartesian coordinate system (x, y, z) with base vectors $(\boldsymbol{e}_x, \boldsymbol{e}_y, \boldsymbol{e}_z)$ is denoted by $\boldsymbol{r}$. An alternate convected coordinate system $(\theta^1, \theta^2, \theta^3)$ with base vectors $(\boldsymbol{g}_1, \boldsymbol{g}_2, \boldsymbol{g}_3)$ is defined such that $(0, 0, \theta^3)$ denotes points on $\mathscr{R}$ (see figure 1). For convenience, we denote θ^3 by ξ and note that, since the θ^1 coordinates are convected, a material particle travelling along the vortex core will always have the same value of ξ.

A vortex core has a certain thickness and spin that must be accounted for in addition to the velocity and position of its axis, where the axis can be taken to correspond with the curve $\mathscr{C}$. If the position vector of any point within the core is $\boldsymbol{p}(\theta^1, \theta^2, \theta^3, t)$, where points on $\mathscr{C}$ are given by $\boldsymbol{p}(0, 0, \theta^3, t) = \boldsymbol{r}(\xi, t)$, we assume that

$$\boldsymbol{p}(\theta^\alpha, \xi, t) = \boldsymbol{r}(\xi, t) + \theta^\alpha \boldsymbol{d}_\alpha(\xi, t). \tag{2.1}$$

In (2.1), $\boldsymbol{d}_\alpha = \boldsymbol{d}_\alpha(\xi, t)$ are called *directors*, $\alpha = (1, 2)$ and the summation convention

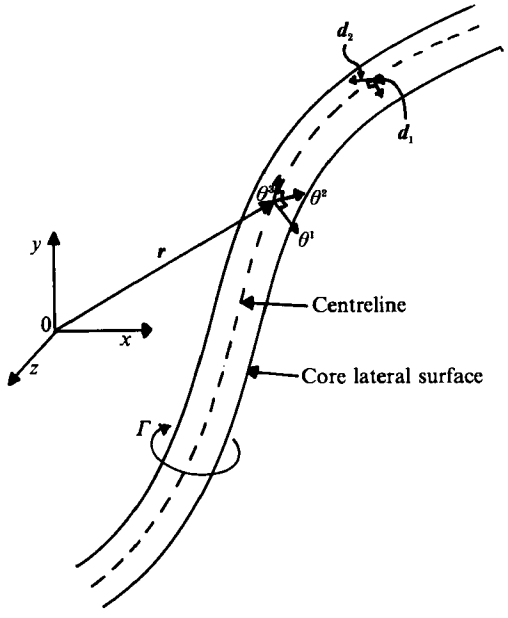

FIGURE 1. Kinematics of vortex core showing fixed coordinate system (x, y, z), convected coordinates $(\theta^1, \theta^2, \theta^3)$, directors $(\boldsymbol{d}_1, \boldsymbol{d}_2)$ and position vector $\boldsymbol{r}$ of the vortex centreline.

over repeated tensor indices is assumed. The base vectors $\boldsymbol{g}_i = \partial \boldsymbol{p}/\partial\theta^i$ can be written using (2.1) as

$$\boldsymbol{g}_\alpha = \boldsymbol{d}_\alpha, \quad \boldsymbol{g}_3 = \partial \boldsymbol{r}/\partial\xi + \theta^\alpha \partial \boldsymbol{d}_\alpha/\partial\xi. \tag{2.2}$$

In the present paper, the directors $\boldsymbol{d}_\alpha$ are chosen to have dimensions of length, so that θ^i are dimensionless and $\boldsymbol{g}_i$ also have dimensions of length, and the magnitude σ of $\boldsymbol{d}_\alpha$ (for either $\alpha = 1, 2$) is identified with the vortex core radius. Because the θ^i coordinate system is convected, the base vectors $\boldsymbol{g}_\alpha$ spin in conjunction with the motion of material line segments spanning the vortex core.

Along the curve $\mathscr{C}$, the base vectors $\boldsymbol{g}_i$ are denoted by $\boldsymbol{a}_i$, where from (2.2) we have

$$\boldsymbol{a}_\alpha = \boldsymbol{d}_\alpha, \quad \boldsymbol{a}_3 = \partial \boldsymbol{r}/\partial\xi, \tag{2.3}$$

and we note that $\boldsymbol{a}_3$ is everywhere tangent to $\mathscr{C}$. The arclength $\mathrm{d}s$ of a material element $\mathrm{d}\xi$ of the directed filament is given by

$$\mathrm{d}s = (a_{33})^{\frac{1}{2}} \mathrm{d}\xi, \tag{2.4}$$

where

$$a_{33} = \boldsymbol{a}_3 \cdot \boldsymbol{a}_3 = g_{33}(\theta^\alpha = 0). \tag{2.5}$$

It is apparent from (2.4) that $(a_{33})^{\frac{1}{2}}$ can be interpreted as the 'stretch' of material line segments along the vortex filament.

It is often convenient to describe the shape of a space curve in terms of its curvature κ and its torsion τ. For this purpose, we define a unit tangent vector $\boldsymbol{\lambda}_3$, a unit principal normal vector $\boldsymbol{\lambda}_1$ and a unit binormal vector $\boldsymbol{\lambda}_2$ of $\mathscr{C}$ by

$$\boldsymbol{\lambda}_3 = \frac{\boldsymbol{a}_3}{(a_{33})^{\frac{1}{2}}} = \frac{\partial \boldsymbol{r}}{\partial s}, \quad \boldsymbol{\lambda}_1 = \frac{\partial \boldsymbol{\lambda}_3/\partial\xi}{|\partial \boldsymbol{\lambda}_3/\partial\xi|}, \quad \boldsymbol{\lambda}_2 = \boldsymbol{\lambda}_3 \times \boldsymbol{\lambda}_1. \tag{2.6}$$

The curvature and torsion may then be obtained from the Serret–Frenet equations

$$\frac{\partial \boldsymbol{\lambda}_3}{\partial s} = \kappa \boldsymbol{\lambda}_1, \quad \frac{\partial \boldsymbol{\lambda}_2}{\partial s} = -\tau \boldsymbol{\lambda}_1, \quad \frac{\partial \boldsymbol{\lambda}_1}{\partial s} = \tau \boldsymbol{\lambda}_2 - \kappa \boldsymbol{\lambda}_3. \tag{2.7}$$

The general equations of motion for a directed filament include equations for mass conservation, conservation of ordinary momentum, balance of director momentum and conservation of angular momentum. The local form of these equations is given by Green *et al.* (1974), using slightly different notation, as

$$\rho(a_{33})^{\frac{1}{2}} = \lambda, \tag{2.8}$$

$$\lambda \dot{\boldsymbol{v}} = \lambda \boldsymbol{f} + \partial \boldsymbol{n}/\partial \xi, \tag{2.9}$$

$$\lambda y^{\alpha\beta} \dot{\boldsymbol{w}}_\beta = \lambda \boldsymbol{l}^\alpha - \boldsymbol{k}^\alpha + \partial \boldsymbol{m}^\alpha/\partial \xi, \tag{2.10}$$

$$\boldsymbol{a}_3 \times \boldsymbol{n} + \boldsymbol{d}_\alpha \times \boldsymbol{k}^\alpha + \partial \boldsymbol{d}_\alpha/\partial \xi \times \boldsymbol{m}^\alpha = \boldsymbol{0}. \tag{2.11}$$

In (2.8), the mass ρ of the vortex filament per unit length is related to the constituent fluid density ρ^* and vortex core radius σ by

$$\rho = \pi \rho^* \sigma^2, \tag{2.12}$$

and $\lambda = \lambda(\xi)$ is the mass of a differential material segment $\mathrm{d}\xi$ of the filament. In (2.9)–(2.10), $\boldsymbol{v} = \dot{\boldsymbol{r}}$ and $\boldsymbol{w}_\alpha = \dot{\boldsymbol{d}}_\alpha$ are the ordinary and director velocities of the filament and the symmetric tensor $y^{\alpha\beta}$ are inertia coefficients, such that the kinetic energy k per unit mass of the filament is

$$k = \tfrac{1}{2}(\boldsymbol{v} \cdot \boldsymbol{v} + y^{\alpha\beta} \boldsymbol{w}_\alpha \cdot \boldsymbol{w}_\beta). \tag{2.13}$$

A superposed dot denotes material derivative keeping ξ fixed, so that for any quantity f,

$$\dot{f} = \mathrm{d}f/\mathrm{d}t = \partial f/\partial t + (\boldsymbol{v} \cdot \boldsymbol{\lambda}_3)\, \partial f/\partial s. \tag{2.14}$$

The forces acting on an element $\mathrm{d}\xi$ of the directed filament, spanning from ξ_0 to $\xi_0 + \mathrm{d}\xi$, include ordinary and director contact forces $\boldsymbol{n}$ and $\boldsymbol{m}^\alpha$, respectively, acting at the end points ξ_0 and $\xi_0 + \mathrm{d}\xi$, ordinary and director assigned forces $\boldsymbol{f}$ and $\boldsymbol{l}^\alpha$ per unit mass acting within $\mathrm{d}\xi$ and an internal director force $\boldsymbol{k}^\alpha$ per unit length acting within $\mathrm{d}\xi$ (see figure 2). The internal force $\boldsymbol{k}^\alpha$ is necessary to account for the fact that director momentum is not conserved. Since in this paper we do not account for the effects of gravity, magnetic forces or other standard 'body' forces, the only contributions to $\boldsymbol{f}$ and $\boldsymbol{l}^\alpha$ come through the external contact forces acting on the lateral boundary of the vortex core.

In general, constitutive equations must be chosen for the response functions $y^{\alpha\beta}$, $\boldsymbol{n}$, $\boldsymbol{m}^\alpha$ and $\boldsymbol{k}^\alpha$ as functions of the independent variables ρ, $\boldsymbol{v}$ and $\boldsymbol{d}^\alpha$ and appropriate rates and gradients of these variables. These equations are usually motivated by an independent weighted-moment approach from the three-dimensional theory, such that the various forces in (2.9)–(2.10) are identified with certain weighted integrals of pressure and velocity gradients across the vortex cross-section or around the vortex circumference (see the Appendix of Caulk & Naghdi 1979). However, before making use of such results, we note that the independent variables are subject to several *constraints*, and we must therefore allow for the existence of indeterminate (or constraint) parts of the response functions.

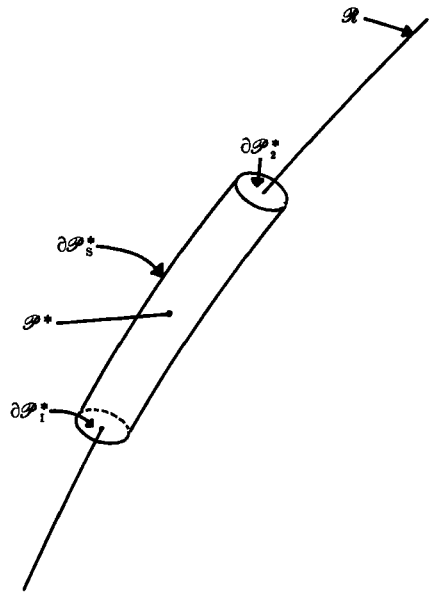

FIGURE 2. Diagram showing a region $\mathscr{P}^*$ of the vortex core with lateral surface $\partial\mathscr{P}_S^*$ and end surfaces $\partial\mathscr{P}_1^*$ and $\partial\mathscr{P}_2^*$. The various forces $\boldsymbol{n}$, $\boldsymbol{m}^\alpha$, $\boldsymbol{f}$, $\boldsymbol{l}^\alpha$, $\boldsymbol{k}^\alpha$, in the directed curve theory may be identified with weighted integrals of forces acting in the three-dimensional theory as follows: (1) the contact forces $\boldsymbol{n}$ and $\boldsymbol{m}^\alpha$ with moments of forces acting on $\partial\mathscr{P}_1^*$ and $\partial\mathscr{P}_2^*$; (2) the forces $\boldsymbol{f}$ and $\boldsymbol{l}^\alpha$ with moments of forces acting on $\partial\mathscr{P}_S^*$ (since no body forces are assumed to be present in the three-dimensional theory); (3) the internal forces $\boldsymbol{k}^\alpha$ with moments of forces acting inside $\mathscr{P}^*$.

There are two constraints which are used in this theory. The first is due to incompressibility of the constituent fluid and can be shown (Caulk & Naghdi 1979) to take the form

$$(e^{\alpha\beta}\boldsymbol{d}_\beta \times \boldsymbol{a}_3)\cdot \boldsymbol{w}_\alpha + (\boldsymbol{d}_1 \times \boldsymbol{d}_2)\cdot \partial v/\partial\xi = 0, \tag{2.15}$$

where $e^{\alpha\beta}$ is the second-order permutation tensor. The second constraint requires that both directors $\boldsymbol{d}_1$ and $\boldsymbol{d}_2$ are oriented normal to the tangent vector $\boldsymbol{a}_3$, or that $\boldsymbol{d}_\alpha\cdot\boldsymbol{a}_3$ vanishes. Taking the material derivative of this constraint, we obtain

$$\boldsymbol{a}_3\cdot\boldsymbol{w}_\alpha + \boldsymbol{d}_\alpha\cdot\partial v/\partial\xi = 0. \tag{2.16}$$

The treatment of the constraint (2.16) is similar to that of Naghdi (1980).

A kinetic energy theorem for the filament can be derived from (2.8)–(2.10) as

$$[\boldsymbol{n}\cdot\boldsymbol{v} + \boldsymbol{m}^\alpha\cdot\boldsymbol{w}_\alpha]_{\xi_1}^{\xi_2} + \int_{\xi_1}^{\xi_2} \lambda(\boldsymbol{f}\cdot\boldsymbol{v} + \boldsymbol{l}^\alpha\cdot\boldsymbol{w}_\alpha)\,\mathrm{d}\xi$$

$$-\frac{\mathrm{d}}{\mathrm{d}t}\int_{\xi_1}^{\xi_2} \tfrac{1}{2}\lambda(\boldsymbol{v}\cdot\boldsymbol{v} + y^{\alpha\beta}\boldsymbol{w}_\alpha\cdot\boldsymbol{w}_\beta)\,\mathrm{d}\xi = \int_{\xi_1}^{\xi_2}\lambda P\,\mathrm{d}\xi, \tag{2.17}$$

where the mechanical power P per unit mass of the filament is defined by

$$\lambda P = \boldsymbol{n}\cdot\partial v/\partial\xi + \boldsymbol{k}^\alpha\cdot\boldsymbol{w}_\alpha + \boldsymbol{m}^\alpha\cdot\partial\boldsymbol{w}_\alpha/\partial\xi. \tag{2.18}$$

If we assume that $\boldsymbol{n}$, $\boldsymbol{m}^\alpha$ and $\boldsymbol{k}^\alpha$ are composed of the sum of constraint parts $\bar{\boldsymbol{n}}, \bar{\boldsymbol{m}}^\alpha$, $\bar{\boldsymbol{k}}^\alpha$ and determinate parts $\hat{\boldsymbol{n}}, \hat{\boldsymbol{m}}^\alpha, \hat{\boldsymbol{k}}^\alpha$, then the usual assumption that the constraints

are 'workless' (Truesdell & Toupin 1960, pp. 600–602) together with (2.18) implies that

$$\bar{\boldsymbol{n}}\cdot\partial\boldsymbol{v}/\partial\xi+\bar{\boldsymbol{k}}^{\alpha}\cdot\boldsymbol{w}_{\alpha}+\bar{\boldsymbol{m}}^{\alpha}\cdot\partial\boldsymbol{w}_{\alpha}/\partial\xi=0. \tag{2.19}$$

From (2.15), (2.16) and (2.19), it follows that $\boldsymbol{n}$, $\boldsymbol{m}^{\alpha}$ and $\boldsymbol{k}^{\alpha}$ have the forms

$$\boldsymbol{n}=\hat{\boldsymbol{n}}-\bar{p}\boldsymbol{d}_1\times\boldsymbol{d}_2+q^{\alpha}\boldsymbol{d}_{\alpha},\quad \boldsymbol{m}^{\alpha}=\hat{\boldsymbol{m}}^{\alpha},\quad \boldsymbol{k}^{\alpha}=\hat{\boldsymbol{k}}^{\alpha}-\bar{p}e^{\alpha\beta}\boldsymbol{d}_{\beta}\times\boldsymbol{a}_3+q^{\alpha}\boldsymbol{a}_3, \tag{2.20}$$

where $\bar{p}=\bar{p}(\xi,t)$ and $q^{\alpha}=q^{\alpha}(\xi,t)$ play the role of Lagrange multipliers resulting from the constraints (2.15) and (2.16), respectively. We note that the result (2.20) satisfies the moment of momentum equation (2.11) identically.

Using the weighted-moment approach from the three-dimensional theory, Caulk & Naghdi (1979) show that if the vortex filament is identified with the vortex axis, then the inertia coefficients are given by

$$y^{12}=y^{21}=0,\quad y^{11}=y^{22}=\tfrac{1}{4}. \tag{2.21}$$

Also, since we are dealing only with inviscid incompressible fluid, the determinate parts $\hat{\boldsymbol{n}}$, $\hat{\boldsymbol{m}}^{\alpha}$ and $\hat{\boldsymbol{k}}^{\alpha}$ all vanish.

Before proceeding further, it is necessary to note some additional kinematical results. It was mentioned previously that the director magnitude is set equal to the core radius and that the directors spin about the vortex axis. We define the vortex 'spin' $\omega=\omega(\xi,t)$ as the axial component of vorticity of a material line spanning the vortex core, so that

$$\mathrm{d}/\mathrm{d}t(\boldsymbol{d}_1/\sigma)=\omega\boldsymbol{d}_2/2\sigma,\quad \mathrm{d}/\mathrm{d}t(\boldsymbol{d}_2/\sigma)=-\omega\boldsymbol{d}_1/2\sigma. \tag{2.22}$$

The circulation Γ of the core is given by

$$\Gamma=\pi\sigma^2\omega, \tag{2.23}$$

and it will be found later that $\Gamma=\Gamma(\xi)$ only, in accord with Kelvin's circulation theorem. From (2.22), we find that the director velocities $\boldsymbol{w}_{\alpha}$ and accelerations $\dot{\boldsymbol{w}}_{\alpha}$ are given by

$$\left.\begin{aligned}\boldsymbol{w}_1&=\dot{\sigma}\boldsymbol{d}_1/\sigma+\tfrac{1}{2}\omega\boldsymbol{d}_2,\quad \boldsymbol{w}_2=\dot{\sigma}\boldsymbol{d}_2/\sigma-\tfrac{1}{2}\omega\boldsymbol{d}_1,\\ \dot{\boldsymbol{w}}_1&=(\ddot{\sigma}/\sigma-\tfrac{1}{4}\omega^2)\,\boldsymbol{d}_1+(\tfrac{1}{2}\dot{\omega}+\dot{\sigma}\omega/\sigma)\,\boldsymbol{d}_2,\quad \dot{\boldsymbol{w}}_2=(\ddot{\sigma}/\sigma-\tfrac{1}{4}\omega^2)\,\boldsymbol{d}_2-(\tfrac{1}{2}\omega+\dot{\sigma}\omega/\sigma)\,\boldsymbol{d}_1.\end{aligned}\right\} \tag{2.24}$$

Substituting (2.20) into (2.9)–(2.10) gives the ordinary and director momentum equations as

$$\lambda\dot{\boldsymbol{v}}=\lambda\boldsymbol{f}+\partial/\partial\xi(q^{\alpha}\boldsymbol{d}_{\alpha}-\bar{p}\boldsymbol{d}_1\times\boldsymbol{d}_2), \tag{2.25a}$$

$$\tfrac{1}{4}\lambda\dot{\boldsymbol{w}}_1=\lambda\boldsymbol{l}_1-q^1\boldsymbol{a}_3+\bar{p}\boldsymbol{d}_2\times\boldsymbol{a}_3, \tag{2.25b}$$

$$\tfrac{1}{4}\lambda\dot{\boldsymbol{w}}_2=\lambda\boldsymbol{l}_2-q^2\boldsymbol{a}_3-\bar{p}\boldsymbol{d}_1\times\boldsymbol{a}_3. \tag{2.25c}$$

In anticipation of the form of $\boldsymbol{l}_{\alpha}$ obtained in the latter part of this section, we assume that

$$\boldsymbol{l}_{\alpha}=l\boldsymbol{d}_{\alpha}/\sigma, \tag{2.26}$$

where l is the magnitude of $\boldsymbol{l}_{\alpha}$. It is now desired to eliminate $\bar{p}$ and q^{α} from (2.25a) with use of (2.25b, c). We first take the scalar product of (2.25b) with $\boldsymbol{d}_1$ or of (2.25c) with $\boldsymbol{d}_2$ (either one gives the same result) and use (2.24) to obtain

$$\tfrac{1}{4}\sigma\lambda(\ddot{\sigma}-\tfrac{1}{4}\omega^2\sigma)=\sigma\lambda l-\bar{p}[\boldsymbol{d}_1\,\boldsymbol{d}_2\,\boldsymbol{a}_3], \tag{2.27}$$

where the scalar triple product in (2.27) is obtained using (2.8) as

$$[\boldsymbol{d}_1\,\boldsymbol{d}_2\,\boldsymbol{a}_3]=\boldsymbol{d}_2\cdot(\boldsymbol{d}_1\times\boldsymbol{a}_3)=-\sigma^2(a_{33})^{\frac{1}{2}}=-\lambda/\pi\rho^{*}. \tag{2.28}$$

Substituting (2.28) into (2.27) and solving for $\bar{p}$ gives

$$\bar{p} = -\pi\rho^*\sigma l + \tfrac{1}{4}\pi\rho^*\sigma(\ddot{\sigma} - \tfrac{1}{4}\omega^2\sigma). \tag{2.29}$$

Next, take the scalar product of (2.25*b*) and (2.25*c*) with $\boldsymbol{a}_3$ to get

$$q^\alpha = 0. \tag{2.30}$$

If we take the scalar product of (2.25*b*) with $\boldsymbol{d}_2$, or of (2.25*c*) with $\boldsymbol{d}_1$, multiply by π and again use (2.24), we obtain the well-known result

$$\pi\sigma(\sigma\dot{\omega} + 2\dot{\sigma}\omega) = \dot{\Gamma} = 0, \tag{2.31}$$

which implies that $\Gamma = \Gamma(\xi)$ only, as stated previously.

It is convenient in what follows to write the velocity $\boldsymbol{v}$ in component form as

$$\boldsymbol{v} = u\boldsymbol{\lambda}_1 + v\boldsymbol{\lambda}_2 + w\boldsymbol{\lambda}_3, \tag{2.32}$$

where $\boldsymbol{\lambda}_1, \boldsymbol{\lambda}_2, \boldsymbol{\lambda}_3$ are defined by (2.6). Taking the material derivative of (2.8) and using (2.12), (2.7), (2.5), (2.3) and (2.32), the mass conservation equation may be written in terms of the components of $\boldsymbol{v}$ in (2.32) as

$$2\dot{\sigma} + \sigma(\partial w/\partial s - \kappa u) = 0. \tag{2.33}$$

Substituting the results (2.29) and (2.30) for $\bar{p}$ and q^α into (2.25*a*) and using (2.7), (2.8) and (2.12), the momentum conservation equations become

$$\sigma^2\dot{\boldsymbol{v}}\cdot\boldsymbol{\lambda}_1 = \sigma^2 f_1 + \kappa\sigma^3\left[l - \frac{1}{4}\left(\ddot{\sigma} - \frac{\Gamma^2}{4\pi^2\sigma^3}\right)\right], \tag{2.34}$$

$$\sigma^2\dot{\boldsymbol{v}}\cdot\boldsymbol{\lambda}_2 = \sigma^2 f_2, \tag{2.35}$$

$$\sigma^2\dot{\boldsymbol{v}}\cdot\boldsymbol{\lambda}_3 = \sigma^2 f_3 + \frac{\partial}{\partial s}(\sigma^3 l - \tfrac{1}{4}\sigma^3\ddot{\sigma}). \tag{2.36}$$

The left-hand sides of (2.34)–(2.36) are given by

$$\dot{\boldsymbol{v}}\cdot\boldsymbol{\lambda}_i = \dot{v}_i + uB_i + vC_i + wA_i, \tag{2.37}$$

where from the Serret–Frenet equations (2.7) we find that

$$\left.\begin{aligned}
&A_1 = \dot{\boldsymbol{\lambda}}_3\cdot\boldsymbol{\lambda}_1 = \partial u/\partial s - \tau v + \kappa w, \quad A_2 = \dot{\boldsymbol{\lambda}}_3\cdot\boldsymbol{\lambda}_2 = \partial v/\partial s + \tau u,\\
&A_3 = \dot{\boldsymbol{\lambda}}_3\cdot\boldsymbol{\lambda}_3 = \partial w/\partial s + 2\dot{\sigma}/\sigma - \kappa u,\\
&B_1 = \dot{\boldsymbol{\lambda}}_1\cdot\boldsymbol{\lambda}_1 = 2\dot{\sigma}/\sigma - \dot{\kappa}/\kappa + (1/\kappa)\,\partial A_1/\partial s - (\tau/\kappa)A_2 + A_3,\\
&B_2 = \dot{\boldsymbol{\lambda}}_1\cdot\boldsymbol{\lambda}_2 = (1/\kappa)\,\partial A_2/\partial s + (\tau/\kappa)A_1, \quad B_3 = \dot{\boldsymbol{\lambda}}_1\cdot\boldsymbol{\lambda}_3 = (1/\kappa)\,\partial A_3/\partial s - A_1,\\
&C_1 = \dot{\boldsymbol{\lambda}}_2\cdot\boldsymbol{\lambda}_1 = (\kappa/\tau)A_1 + (1/\tau)\,\partial B_1/\partial s - B_2 + \kappa/\tau B_3,\\
&C_2 = \dot{\boldsymbol{\lambda}}_2\cdot\boldsymbol{\lambda}_2 = (\kappa/\tau)A_2 - \dot{\tau}/\tau - 2\dot{\sigma}/\sigma + (1/\tau)\,\partial B_2/\partial s + B_1,\\
&C_3 = \dot{\boldsymbol{\lambda}}_2\cdot\boldsymbol{\lambda}_3 = \dot{\kappa}/\tau + (\kappa/\tau)A_3 - (2\dot{\sigma}/\sigma)\kappa/\tau + (1/\tau)\,\partial B_3/\partial s - (\kappa/\tau)B_1.
\end{aligned}\right\} \tag{2.38}$$

It is noted, however, that since $\boldsymbol{\lambda}_1$, $\boldsymbol{\lambda}_2$ and $\boldsymbol{\lambda}_3$ are unit vectors, A_3, B_1 and C_2 in (2.38) must vanish. Setting A_3 equal to zero yields the mass conservation equation (2.33) and setting B_1 and C_2 equal to zero yields

$$\dot{\kappa}/\kappa = 2\dot{\sigma}/\sigma + (1/\kappa)\,\partial A_1/\partial s - (\tau/\kappa)A_2, \quad \dot{\tau}/\tau = 2\dot{\sigma}/\sigma + (\kappa/\tau)A_2 + (1/\tau)\,\partial B_2/\partial s. \tag{2.39}$$

The results (2.33)–(2.36) provide equations for determination of σ, u, v, w, given the

assigned force fields $\boldsymbol{f}$ and $\boldsymbol{l}^\alpha$, and the kinematic results (2.39) provide equations for determination of κ and τ.

2.2. *Assigned (external) forces* $\boldsymbol{f}$ *and* $\boldsymbol{l}^\alpha$

The ordinary and director assigned forces $\boldsymbol{f}$ and $\boldsymbol{l}^\alpha$ are related, respectively, to the integral and the first moment of pressure about the lateral core surface ∂A. Letting the unit normal of the core surface ∂A be denoted by $\boldsymbol{\nu}^*$, the stress vector $\boldsymbol{t}$ acting on ∂A is given by

$$\boldsymbol{t} = \boldsymbol{T}^i \nu_i^* g^{-\frac{1}{2}}, \quad \boldsymbol{\nu}^* = \nu_i^* \boldsymbol{g}^i, \tag{2.40}$$

where $g^{\frac{1}{2}} = (\det \boldsymbol{g}_i \cdot \boldsymbol{g}_j)^{\frac{1}{2}}$ and the base vectors $\boldsymbol{g}_i$ are defined in (2.2). The assigned forces can then be obtained as (Caulk & Naghdi 1979)

$$\lambda \boldsymbol{f} = \int_{\partial A} (\boldsymbol{T}^1 \,\mathrm{d}\theta^2 - \boldsymbol{T}^2 \,\mathrm{d}\theta^1), \quad \lambda \boldsymbol{l}^\alpha = \int_{\partial A} \theta^\alpha (\boldsymbol{T}^1 \,\mathrm{d}\theta^2 - \boldsymbol{T}^2 \,\mathrm{d}\theta^1), \tag{2.41}$$

and for an inviscid fluid $\boldsymbol{T}^1$ and $\boldsymbol{T}^2$ are proportional to pressure along the core surface.

Prior to calculation of $\boldsymbol{f}$ and $\boldsymbol{l}^\alpha$ from (2.41), it is necessary to introduce some assumption for the exterior flow field. It is thus assumed that in a region of radius R, where $R \gg \sigma$, about the vortex core the exterior flow is irrotational and consists of some combination of the following four components: (i) a circumferential velocity $\Gamma/2\pi r$, corresponding to a potential vortex, (ii) a radial velocity $m/2\pi r$, where $m = m(s,t)$, corresponding to a line source, (iii) a prescribed uniform velocity $\boldsymbol{u}_{\mathrm{E}}$, (iv) an induced uniform velocity $\boldsymbol{u}_{\mathrm{B}}$. The total uniform velocity past the core is given by $\boldsymbol{u} = \boldsymbol{u}_{\mathrm{E}} + \boldsymbol{u}_{\mathrm{B}}$. The induced velocity $\boldsymbol{u}_{\mathrm{B}}$ may be calculated in general by the Biot–Savart law with cutoff (see MS or LA), but in many cases we simply use the local-induction approximation of Arms & Hama (1965) in the form

$$\boldsymbol{u}_{\mathrm{B}}(s,t) = (\Gamma\kappa/4\pi)[\ln(1/\kappa\sigma) + C]\,\boldsymbol{\lambda}_2, \tag{2.42}$$

where C is a constant of order unity. It is also noted that the assumption that the prescribed velocity $\boldsymbol{u}_{\mathrm{E}}$ is uniform can be approximately satisfied whenever the typical lengthscale L over which velocity changes in the prescribed external flow is much greater than the core radius σ. In the presence of the uniform external velocity $\boldsymbol{u}$, the relative normal velocity $\boldsymbol{q}$ to the vortex filament is given by

$$\boldsymbol{q} = (\boldsymbol{u} - \boldsymbol{v}) - [(\boldsymbol{u} - \boldsymbol{v}) \cdot \boldsymbol{\lambda}_3]\,\boldsymbol{\lambda}_3, \tag{2.43}$$

where $\boldsymbol{v}$ is the filament velocity introduced previously.

An expression for the ordinary assigned force $\boldsymbol{f}$ on the vortex filament is now given as

$$\pi\sigma^2 \boldsymbol{f} = \Gamma \boldsymbol{q} \times \boldsymbol{\lambda}_3 + \pi\sigma\,\delta/\delta t(\sigma \boldsymbol{q}) + \pi\sigma\,\delta/\delta t[\sigma \boldsymbol{u} - \sigma \boldsymbol{\lambda}_3 (\boldsymbol{u} \cdot \boldsymbol{\lambda}_3)] - \pi\sigma l\,\partial/\partial s(\sigma^2 \boldsymbol{\lambda}_3). \tag{2.44}$$

Equation (2.44) is a slight modification of that derived by MS and is valid under the assumptions $\kappa\sigma \ll 1$ and $\sigma/L \ll 1$, where L is the typical lengthscale of either of the exterior flow components (iii) or (iv) listed previously. The first term in (2.44) is the Kutta lift force obtained when a solid cylinder of radius σ spinning with circulation Γ travels with velocity $\boldsymbol{q}$ through a still fluid. It is of note that when a vortex filament is bent, the Kutta lift caused by the induced velocity field $\boldsymbol{u}_{\mathrm{B}}$ will act to resist bending and restore the vortex to a columnar position. The similarities between this effect and bending tension in solid rods is discussed by MS.

The second and third terms in (2.44) are usually referred to as 'added mass' force and 'buoyancy' force, respectively, although it may perhaps be more convenient

simply to refer to the sum of the two as inertial drag. The time derivative $\delta f/\delta t$ in (2.44), for some quantity f, represents the rate of change of f as measured by an observer travelling with the exterior velocity $\boldsymbol{u}$ and is defined by

$$\delta f/\delta t = \partial f/\partial t + (\boldsymbol{u}\cdot\boldsymbol{\lambda}_3)\,\partial f/\partial s = \dot{f} + [(\boldsymbol{u}-\boldsymbol{v})\cdot\boldsymbol{\lambda}_3]\,\partial f/\partial s. \tag{2.45}$$

Added mass force should exist both when $\boldsymbol{q}$ changes with time, so that the core has a non-zero acceleration relative to the external flow, or when σ changes in time, in which case the core acts like a mass source or sink in a uniform flow $\boldsymbol{q}$. LA assumes an added mass force proportional to $\sigma^2\delta\boldsymbol{q}/\delta t$, which neglects the latter effect. MS assume an added mass force of the form $\mathrm{d}(\sigma^2\boldsymbol{q})/\mathrm{d}t$ but because they are interested primarily in constant-area vortices, they later neglect this term. The form of the inertial forces used in (2.44), although slightly different from those used by LA and MS, is derived by a careful analysis of the problem of irrotational flow past a cylinder where the cylinder radius, the cylinder velocity and the external flow velocity all vary in time. Some useful expansions of the inertial drag in terms of the coefficients defined in (2.38) are given in the Appendix.

The last term in (2.44) is caused by the exterior pressure (incorporated in l) acting on a gradient in core area, and for steady straight vortices this term is the same as the 'axial force' discussed by LA. For curved vortices, a part of this term acts in the $\boldsymbol{\lambda}_1$ direction (due to a gradient in $\boldsymbol{\lambda}_3$), but this part is cancelled by a constraint force in (2.34) and has no dynamical significance.

We now turn to calculation of the director-assigned force $\boldsymbol{l}^{\alpha}$. It has previously been stated that the present theory considers only circular vortices, and yet the pressure field set up by uniform flow $\boldsymbol{q}$ past the core will tend to make the core non-circular. We must therefore assume that the circumferential velocity is much larger than $|\boldsymbol{q}|$, and hence in calculation of $\boldsymbol{l}^{\alpha}$ only the circumferential and radial components (i) and (ii) of the external flow field are considered. The unsteady Bernoulli equation (in the three-dimensional theory) can then be used to determine the pressure on the lateral core boundary as

$$p_{\mathrm{s}} = -\tfrac{1}{2}\rho^*\left(\frac{\Gamma^2}{4\pi^2\sigma^2} + \left(\frac{\delta\sigma}{\delta t}\right)^2\left[3 + 2\ln\left(\frac{\sigma}{\sigma_0}\right)\right]\right). \tag{2.46}$$

In (2.46), the source strength $m = 2\pi\sigma(\delta\sigma/\delta t)$ (which follows from assuming the no-penetration condition on the core boundary), σ_0 is some reference core radius and the pressure is assumed to approach zero at infinity. Expressions for $\boldsymbol{l}^{\alpha}$ are obtained using (2.41) which have the form (2.26) with l given by

$$l = -\frac{p_{\mathrm{s}}}{\rho^*\sigma} = \frac{\Gamma^2}{8\pi^2\sigma^3} + \frac{1}{2\sigma}\left(\frac{\delta\sigma}{\delta t}\right)^2\left[3 + 2\ln\left(\frac{\sigma}{\sigma_0}\right)\right]. \tag{2.47}$$

It is noted that for constant σ and for $\boldsymbol{u}\cdot\boldsymbol{\lambda}_3 = 0$, the final equations governing vortex motion in the present theory are found to be identical, apart from notation, to those of LA, even though our approach was much different. When σ is not constant, the equations of the present theory differ somewhat from those of LA; however, most of the differences can be traced to the effects of radial inertia, which LA neglects.

3. Some elementary solutions

3.1. *Vortex ring*

The classic solution by WB for a steady vortex ring with axial velocity w, namely

$$v = \frac{\Gamma\kappa}{4\pi}\left[\ln\left(\frac{8}{\kappa\sigma}\right) - \frac{1}{4}\right] - \frac{\pi\sigma^2\kappa w^2}{\Gamma}, \tag{3.1}$$

can be obtained from the momentum equation (2.34) with induced velocity $\boldsymbol{u}_{\mathrm{B}}$ given by

$$\boldsymbol{u}_{\mathrm{B}} = (\Gamma\kappa/4\pi)[\ln(8/\kappa\sigma) - \tfrac{1}{2}]\,\boldsymbol{\lambda}_2. \tag{3.2}$$

The expression (3.2) for induced velocity follows from the local induction approximation (2.42) with $C = \ln(8) - \frac{1}{2}$ and is the same as that used by MS. LA add to (3.2) an additional term $(\Gamma\kappa/16\pi)\,\boldsymbol{\lambda}_2$, which is supplied by an internal constraint force in the present theory.

3.2. *Helical waves*

A helical wave with displacement amplitude D, 'pitch' γD, wavenumber γ and axis along the z-direction is specified by

$$\left.\begin{aligned} &\boldsymbol{r} = D\boldsymbol{e}_r - \gamma Dz\boldsymbol{e}_\theta + z\boldsymbol{e}_z, \quad \boldsymbol{\lambda}_1 = -\boldsymbol{e}_r, \quad \boldsymbol{\lambda}_2 = -\frac{\boldsymbol{e}_\theta + \gamma D\boldsymbol{e}_z}{(1+\gamma^2D^2)^{\frac{1}{2}}}, \\ &\boldsymbol{\lambda}_3 = \frac{-\gamma D\boldsymbol{e}_\theta + \boldsymbol{e}_z}{(1+\gamma^2D^2)^{\frac{1}{2}}}, \quad \kappa = \frac{D\gamma^2}{1+\gamma^2D^2}, \quad \tau = \pm\frac{\gamma}{1+\gamma^2D^2}. \end{aligned}\right\} \tag{3.3}$$

For a steady wave with $u = 0$ and uniform σ, w and v along the vortex length, the momentum equation (2.34) yields a solution for the velocity component v as

$$v = \frac{\kappa}{4\tau^2}\left(\tau w_{\mathrm{B}} + 2\tau w + \frac{2\tau^2}{\kappa}v_{\mathrm{B}} - \frac{\Gamma}{\pi\sigma^2}\right)$$

$$\pm\frac{\kappa}{4\tau^2}\left[\left(\tau w_{\mathrm{B}} + 2\tau w + \frac{2\tau^2}{\kappa}v_{\mathrm{B}} - \frac{\Gamma}{\pi\sigma^2}\right)^2 - \left(8\tau^2w^2 + \frac{16\tau^3}{\kappa}w_{\mathrm{B}}v_{\mathrm{B}} - \frac{8\tau^2\Gamma v_{\mathrm{B}}}{\pi\sigma^2\kappa} - \frac{\tau^2\Gamma^2}{2\pi^2\sigma^2}\right)\right]^{\frac{1}{2}}, \tag{3.4}$$

where we set

$$\boldsymbol{u}_{\mathrm{B}} = u_{\mathrm{B}}\boldsymbol{\lambda}_1 + v_{\mathrm{B}}\boldsymbol{\lambda}_2 + w_{\mathrm{B}}\boldsymbol{\lambda}_3. \tag{3.5}$$

The classic solution of a helix with small pitch, $\gamma D \ll 1$ (Kelvin 1880), can be obtained from (3.4) by setting

$$v_{\mathrm{B}} = \frac{\Gamma\gamma^2D}{4\pi}\left[\ln\left|\frac{2}{\gamma\sigma}\right| - c_{\mathrm{e}}\right], \quad w_{\mathrm{B}} = 0, \quad c_{\mathrm{e}} = 0.5772\ldots, \tag{3.6}$$

and linearizing appropriately. In the other extreme of very large pitch ($\gamma D \to \infty$), the solution for v in (3.4) approaches the vortex ring solution (3.1). (The author is grateful to a referee for suggesting this limit.)

For large values of γD, it is found that the induced velocity $\boldsymbol{u}_{\mathrm{B}}$ may be neglected in (3.4) so long as $(\gamma\sigma)^2 \ll 1$, where we assume that $v_{\mathrm{B}} = O(\Gamma\gamma^2D) \geqslant O(w_{\mathrm{B}})$. This case, which might be called a 'no-induction' approximation, would correspond to a typical situation in which $\gamma D \leqslant O(1)$ and $D/\sigma \gg 1$, and it seems to agree with an observation

made by LA to the effect that the induced velocity had little effect on their numerical computations of unsteady helical waves of finite pitch. Thus neglecting v_B and w_B and defining a 'swirl number' $\Omega = 2\pi w\sigma/\Gamma$, the solution (3.4) for v may be written as

$$\frac{2\pi v\sigma}{\Gamma} = \frac{\kappa}{2\tau}\left(\Omega - \frac{1}{\tau\sigma}\right) \pm \frac{\kappa}{2\tau}\left[\frac{1}{\tau^2\sigma^2} + \tfrac{1}{2} - \Omega^2 - \frac{2\Omega}{\tau\sigma}\right]^{\frac{1}{2}}. \tag{3.7}$$

The solution (3.7) is the same (except for notation) as that given by LA in the absence of induced velocity. Since we expect $\tau = O(\gamma)$, it follows from our previous assumption $(\gamma\sigma)^2 \ll 1$ and from (3.7) that v is imaginary (which implies that a steady helical wave cannot exist) whenever

$$\Omega > (\sqrt{2}-1)/\tau\sigma \quad \text{or} \quad \Omega < -(\sqrt{2}+1)/\tau\sigma. \tag{3.8}$$

The results (3.8) are the same as the criteria found by WB for instability of a straight vortex with axial flow.

3.3. *Axisymmetric solitary waves*

The problem of axisymmetric waves on a vortex core is considered in this section with the simplifying assumptions of a straight vortex filament and a stationary wave field with no external axial flow, for which case (2.34)–(2.35) are satisfied identically and (2.33) and (2.36) become

$$2w\sigma' + \sigma w' = 0, \tag{3.9a}$$

$$\sigma^2 w w' = -\frac{\Gamma^2\sigma'}{4\pi^2\sigma} - \tfrac{1}{4}\sigma^2 w[\sigma\sigma' w' + \sigma w\sigma'']', \tag{3.9b}$$

where a prime denotes differentiation with respect to s. Integrating (3.9a, b) gives

$$\pi w\sigma^2 = Q, \tag{3.10a}$$

$$\frac{Q^2}{\pi^2\sigma^2} + \frac{\Gamma^2}{4\pi^2}\ln\left(\frac{\sigma}{\sigma_0}\right) - \frac{Q^2}{4\pi^2}\left[\frac{2(\sigma')^2}{\sigma^2} - \frac{\sigma''}{\sigma}\right] = S, \tag{3.10b}$$

where Q and S are constants of integration and σ_0 is the equilibrium core radius. Multiplying (3.10b) by $8\pi^2\sigma'/Q^2\sigma^3$ and integrating again, we obtain

$$(\sigma')^2 + q(\sigma) = 0, \tag{3.11}$$

where

$$q(\sigma) = R\sigma^4 - \frac{\Gamma^2\sigma^2}{Q^2}\left[\ln\left(\frac{\sigma}{\sigma_0}\right) + \tfrac{1}{2}\right] + \frac{4\pi^2 S\sigma^2}{Q^2} - 2 \tag{3.12}$$

and R is another constant of integration.

For a solitary wave, σ' and σ'' must vanish far from the wave peak (as $\sigma \to \sigma_0$) so that from (3.10)–(3.12) we obtain

$$R = \frac{\Gamma^2}{2Q^2\sigma_0^2} - \frac{2}{\sigma_0^4}, \quad S = \frac{Q^2}{\pi^2\sigma_0^2}. \tag{3.13}$$

Since $(\sigma')^2$ is non-negative for all real σ', it follows from (3.11) that $q(\sigma)$ must be non-positive for all admissible values of σ. Also, since the peak of the solitary wave coincides with a local maximum in σ, from (3.11) we find that the maximum core radius $\sigma_{\max}$ must be a root of $q(\sigma)$.

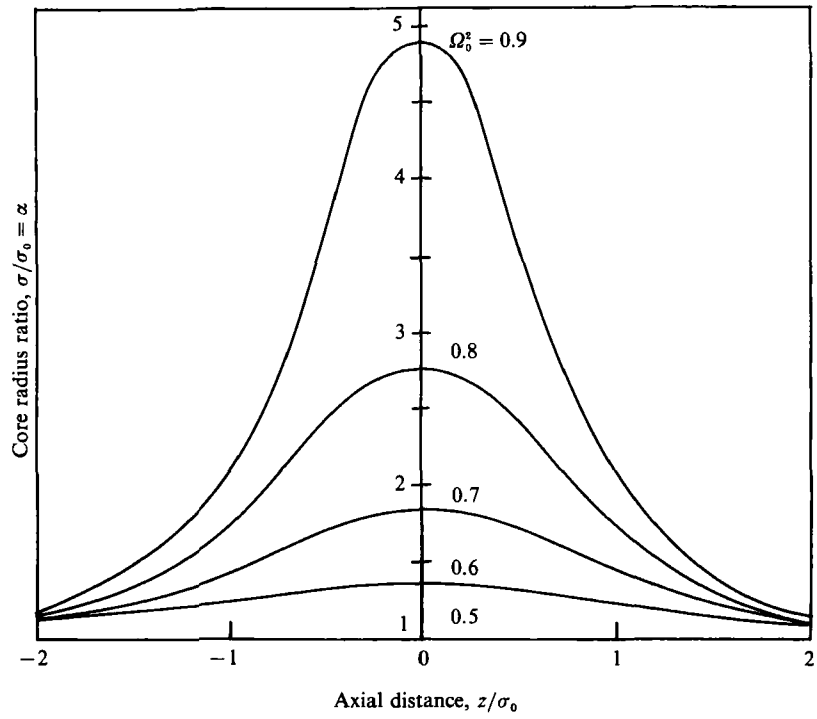

FIGURE 3. Core radius profiles of stationary axisymmetric solitary waves for various Ω_0^2, calculated from (3.11) and (3.14).

Defining the equilibrium swirl number by $\Omega_0 = 2\pi\sigma_0 w_0/\Gamma_0$, which is the value of Ω in the absence of axisymmetric waves, then $q(\sigma)$ in (3.12) may be rewritten using (3.13) as

$$q(\alpha) = 2\left(\frac{1}{\Omega_0^2}-1\right)\alpha^4 - 4\left(\frac{1}{\Omega_0^2}[\ln(\alpha)+\tfrac{1}{2}]-1\right)\alpha^2 - 2, \tag{3.14}$$

where $\alpha = \sigma/\sigma_0$ is the core radius ratio. The equilibrium solution $\alpha = 1$ is a root of q for all values of Ω_0^2; however, in order for a solitary wave to exist there must be some real root $\alpha_{\max} > 1$ of q, and q must be negative for $1 < \alpha < \alpha_{\max}$. Using (3.14), it is thus found that stationary solitary waves are possible if and only if Ω_0^2 lies in the range

$$\tfrac{1}{2} < \Omega_0^2 < 1. \tag{3.15}$$

The wave profile is calculated numerically using (3.11) and (3.14) and is plotted in figure 3 for various values of Ω_0^2. For Ω_0^2 greater than about 0.8, the wave appears to be quite peaked, and it may be expected to become unstable for Ω_0^2 sufficiently near 1; however, the instability problem is not pursued in this paper. An asymptotic solution for α as $\Omega_0^2 \to 0.5$ can be found from (3.11) and (3.14), using standard procedures, as

$$\alpha = \frac{\sigma}{\sigma_0} = 1 + \frac{3}{2}\left(1-\frac{1}{2\Omega_0^2}\right)\operatorname{sech}^2\left[\frac{z}{\sigma_0}\left(2-\frac{1}{\Omega_0^2}\right)^{\frac{1}{2}}\right]. \tag{3.16}$$

Equation (3.16) is similar to the standard sech^2 solution for solitary surface waves in shallow water, and it appears to be of the same form as the solution of Benjamin (1967) for moderately small-amplitude axisymmetric waves on straight vortices. A

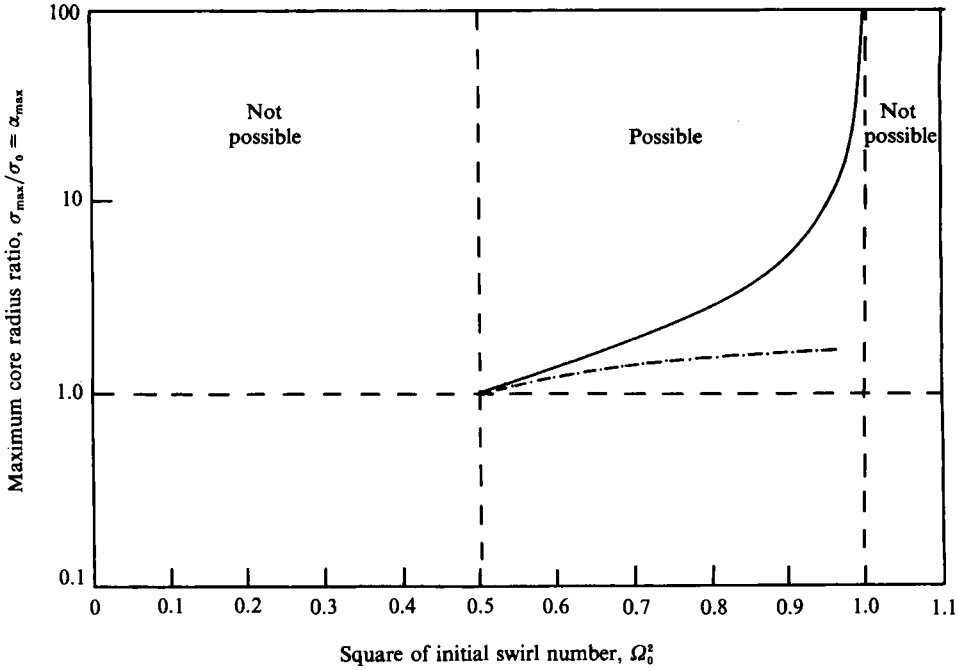

FIGURE 4. Amplitudes of stationary axisymmetric solitary waves as a function of Ω_0^2 and regions in which such waves can and cannot exist: ——, numerical solution from (3.14); —·—·—, asymptotic solution from (3.16) for $\Omega_0^2 \to 0.5$.

comparison between the values of α_{max} predicted by the asymptotic solution (3.16) and the full equation (3.14) for $q(\alpha)$ is given in figure 4, and it is found that the solution (3.16) deviates considerably from the exact solution for $\Omega_0^2 > 0.6$.

4. Vortex breakdown

A 'vortex breakdown' is a point at which the vortex undergoes a sudden transition from one state to another. The phenomenon is in many ways analogous to a hydraulic jump (Benjamin 1962, 1967) or to a shock in gas dynamics (LA). A vortex core may exhibit two major types of breakdowns – helical and axisymmetric – although variations of these types have been observed (Sarpkaya 1971). In axisymmetric breakdowns, a large 'breakdown bubble' forms with a complicated and often turbulent flow inside. A straight vortex section is observed downstream of the bubble, which may later transform into a helical wave. In helical breakdowns, the core undergoes a sudden (almost instantaneous) transition from a straight vortex to a helical wave, and the helix appears to have a nearly constant radius immediately after the breakdown. Helical breakdown differs from helical instability of a straight vortex in that there seems to be no observable slow growth of unstable helical waves, but rather a rapid transition from one fully developed state to another.

In this paper, we model both types of vortex breakdowns as discontinuity points on the vortex (an idea first suggested by LA). For helical breakdowns, such a model seems to be quite appropriate; however, for axisymmetric breakdowns the 'shock' model may be too simplistic in many cases. For instance, when a large breakdown bubble exists, the shock model is clearly inappropriate in cases where the flow upstream is unsteady because the model predicts instantaneous transmission of

information across the bubble, which is not realistic. For such cases, which will not be considered here, it may be more appropriate to formulate a model similar to that used for acoustic wave propagation through a cavity. Secondly, it is well known that the bounding surface of the breakdown bubble is not material and that fluid streams into the downstream side and out of the upstream side. It is thus not entirely clear that the assumption of mass conservation at the 'shock' is justified. However, for axisymmetric breakdowns with uniform-core vortex sections, the predictions of LA (who assume mass conservation at the 'shock') compare well with data, and we shall also make this assumption in the present paper.

4.1. *General jump conditions*

A point of discontinuity P is assumed to exist on the vortex filament for all time t. The velocity $\boldsymbol{V}$ of P is given by

$$\boldsymbol{V} = u\boldsymbol{\lambda}_1 + v\boldsymbol{\lambda}_2 + W\boldsymbol{\lambda}_3,$$

so that $\boldsymbol{V}$ and the velocity $\boldsymbol{v}$ of a material particle at P differ at most by the axial component. The jump conditions across P can be derived from the global balance laws of the filament (Caulk & Naghdi 1979) and are given by

$$\left.\begin{gathered}[\![\rho(w-W)]\!] = 0, \quad [\![\rho(w-W)\,\boldsymbol{v}-\boldsymbol{n}]\!] = \boldsymbol{F}, \quad [\![\rho(w-W)\,y^{\alpha\beta}\boldsymbol{w}_\beta - \boldsymbol{m}^\alpha]\!] = \boldsymbol{L}^\alpha, \\ [\![\rho k(w-W) - \boldsymbol{n}\cdot\boldsymbol{v} - \boldsymbol{m}^\alpha\cdot\boldsymbol{w}_\alpha]\!] = \Phi + \boldsymbol{F}\cdot\boldsymbol{V} + \boldsymbol{L}^\alpha\cdot\boldsymbol{W}_\alpha,\end{gathered}\right\} \tag{4.1}$$

where the notation $[\![f]\!] = f^+ - f^-$ for any quantity f. The terms $\boldsymbol{F}$, $\boldsymbol{L}^\alpha$ and Φ on the right-hand sides of (4.1) represent the supply rates to the discontinuity of ordinary and director momentum and of kinetic energy, respectively. The internal energy term usually appearing in the energy jump condition has been lumped together with Φ, and we interpret $-\Phi$ as the energy dissipation rate at P and $\boldsymbol{F}\cdot\boldsymbol{V} + \boldsymbol{L}^\alpha\cdot\boldsymbol{W}_\alpha$ as the rate of work supplied to P by external forces. The director velocity $\boldsymbol{W}_\alpha$ associated with the discontinuity point P may be related to the rate of change of the breakdown bubble radius and is found to vanish in nearly all cases of interest. The mass, momentum and energy jumps in (4.1) may be rewritten with $\boldsymbol{W}_\alpha = \boldsymbol{0}$ and using the various results (2.12), (2.13), (2.20), (2.24) and (2.29) for ρ, k, $\boldsymbol{n}$, $\boldsymbol{m}^\alpha$ and $\boldsymbol{w}_\alpha$ as

$$[\![\sigma^2(w-W)]\!] = 0, \tag{4.2a}$$

$$\left[\!\!\left[\sigma^2(w-W)\,\boldsymbol{v} - \left(\sigma^3 l - \tfrac{1}{4}\sigma^3\ddot{\sigma} + \frac{\Gamma^2}{16\pi^2}\right)\boldsymbol{\lambda}_3\right]\!\!\right] = \frac{\boldsymbol{F}}{\pi\rho^*}, \tag{4.2b}$$

$$\left[\!\!\left[\tfrac{1}{2}\sigma^2(w-W)\left(u^2+v^2+w^2+\tfrac{1}{2}(\dot{\sigma})^2 + \frac{\Gamma^2}{8\pi^2\sigma^2}\right) - w\left(\sigma^3 l - \tfrac{1}{4}\sigma^3\ddot{\sigma} + \frac{\Gamma^2}{16\pi^2}\right)\right]\!\!\right] = \frac{1}{\pi\rho^*}(\Phi + \boldsymbol{F}\cdot\boldsymbol{V}). \tag{4.2c}$$

4.2. *Axisymmetric vortex breakdowns*

The rate $\boldsymbol{F}$ of momentum supply to the discontinuity is assumed to be a result of an integrable singularity in the external assigned force $\boldsymbol{f}$ at P. Letting s_0^- be a point just below and s_0^+ a point just above the discontinuity point P, located at s_0, we can then write

$$\boldsymbol{F} = \int_{s_0^-}^{s_0^+} \rho\boldsymbol{f}\,\mathrm{d}s. \tag{4.3}$$

For a straight vortex with no axial external flow, substitution of (2.44) into (4.3) gives

$$\boldsymbol{F} = -(\rho^*\Gamma^2/4\pi)[\![\ln(\sigma)]\!]\,\boldsymbol{\lambda}_3, \tag{4.4}$$

where Γ is continuous across the jump.

For a straight vortex $u = v = 0$ and, after using (4.4) and the result (2.47) for l, the jump conditions (4.2) become

$$[\![\sigma^2(w-W)]\!] = 0, \tag{4.5a}$$

$$\left[\!\!\left[\sigma^2 w(w-W)+\tfrac{1}{4}\sigma^3\ddot{\sigma}-\tfrac{1}{2}\sigma^2\left(\frac{\partial\sigma}{\partial t}\right)^2\left\{3+2\ln\left(\frac{\sigma}{\sigma_0}\right)\right\}\right]\!\!\right] = -\frac{\Gamma^2}{4\pi^2}\left[\!\!\left[\ln\left(\frac{\sigma}{\sigma_0}\right)\right]\!\!\right], \tag{4.5b}$$

$$\left[\!\!\left[\tfrac{1}{2}\sigma^2(w-W)\left\{w^2+\tfrac{1}{2}(\dot{\sigma})^2+\frac{\Gamma^2}{8\pi^2\sigma^2}\right\}-\frac{3\Gamma^2 w}{16\pi^2}+\tfrac{1}{4}\sigma^3\ddot{\sigma}w\right.\right.$$

$$\left.\left.-\tfrac{1}{2}\sigma^2 w\left(\frac{\partial\sigma}{\partial t}\right)^2\left\{3+2\ln\left(\frac{\sigma}{\sigma_0}\right)\right\}\right]\!\!\right] = \frac{\Phi}{\pi\rho^*}-\frac{\Gamma^2}{4\pi^2}W\left[\!\!\left[\ln\left(\frac{\sigma}{\sigma_0}\right)\right]\!\!\right]. \tag{4.5c}$$

Equations (4.5*a*, *b*) can be used to solve for W and the jump in $\dot{w}$ across the discontinuity and (4.5*c*) can then be used to solve for Φ. Also, in what follows we assume, as a necessary condition for vortex breakdown to exist, that the energy dissipation rate must be positive. When $w > 0$, this condition implies that $\Phi \leqslant 0$.

The typical axisymmetric vortex breakdown is observed to occur between two sections of approximately uniform, but different, core radius. Setting $\partial\sigma/\partial s = \partial\sigma/\partial t = 0$ in (4.5) and solving for W, w_2 and Φ (where the subscripts 1 and 2 denote the upstream and downstream sides of the jump, respectively, assuming that $w \geqslant 0$) gives

$$W = w_1 \pm \frac{\Gamma\sigma_2}{2\pi\sigma_1}\left[\frac{\ln(\sigma_2/\sigma_1)}{\sigma_2^2-\sigma_1^2}\right]^{\frac{1}{2}}, \tag{4.6a}$$

$$w_2 = w_1 \pm \frac{\Gamma}{2\pi\sigma_1\sigma_2}\left[(\sigma_2^2-\sigma_1^2)\ln\left(\frac{\sigma_2}{\sigma_1}\right)\right]^{\frac{1}{2}}, \tag{4.6b}$$

$$\frac{\Phi}{\pi\rho^*} = \mp\frac{\Gamma^3}{16\pi^3\sigma_1\sigma_2}(\sigma_2^2-\sigma_1^2)^{\frac{1}{2}}\ln^{\frac{1}{2}}\left(\frac{\sigma_2}{\sigma_1}\right)\left[1+\ln\left(\frac{\sigma_2}{\sigma_1}\right)\right]\pm\frac{\Gamma^3\sigma_2}{16\pi^3\sigma_1}\frac{\ln^{\frac{3}{2}}(\sigma_2/\sigma_1)}{(\sigma_2^2-\sigma_1^2)^{\frac{1}{2}}}. \tag{4.6c}$$

For each (σ_1, σ_2) pair, there are two values each of W, w_2 and Φ, corresponding to left- and right-running shocks. Equations (4.6*a*, *b*) are identical (apart from notation) to the results obtained by LA, and a comparison between the predictions of (4.6*a*, *b*) and experimental data of Garg & Leibovich (1979) is given by LA, showing fairly good agreement.

For a stationary shock, we set $W = 0$ in (4.6) to obtain equations for σ_2/σ_1 and Φ as

$$(1-\sigma_1^2/\sigma_2^2)\,\Omega_1^2 = \ln(\sigma_2/\sigma_1), \tag{4.7}$$

$$-\frac{16\pi^2\sigma_1\Phi}{\rho^*\Gamma^3\Omega_1} = \left(1-\frac{\sigma_1^2}{\sigma_2^2}\right)\left[\left(1+\frac{\sigma_1^2}{\sigma_2^2}\right)\Omega_1^2-1\right], \tag{4.8}$$

where $\Omega_1 = 2\pi w_1\sigma_1/\Gamma$ is the upstream swirl number. Values of σ_2/σ_1 and $-16\pi^2\sigma_1\Phi/\rho^*\Gamma^3\Omega_1$ from (4.7)–(4.8) are plotted versus Ω_1^2 in figure 5. It is noted that the existence condition $\Phi \leqslant 0$ yields

$$\Omega_1^2 \geqslant \tfrac{1}{2} \tag{4.9}$$

as a necessary condition for stationary vortex breakdowns of this type. The energy dissipation rate in figure 5 for Ω_1^2 in the range $\frac{1}{2} < \Omega_1^2 < 1$ is very small, and so the breakdown bubble might also be expected to be small in this range.

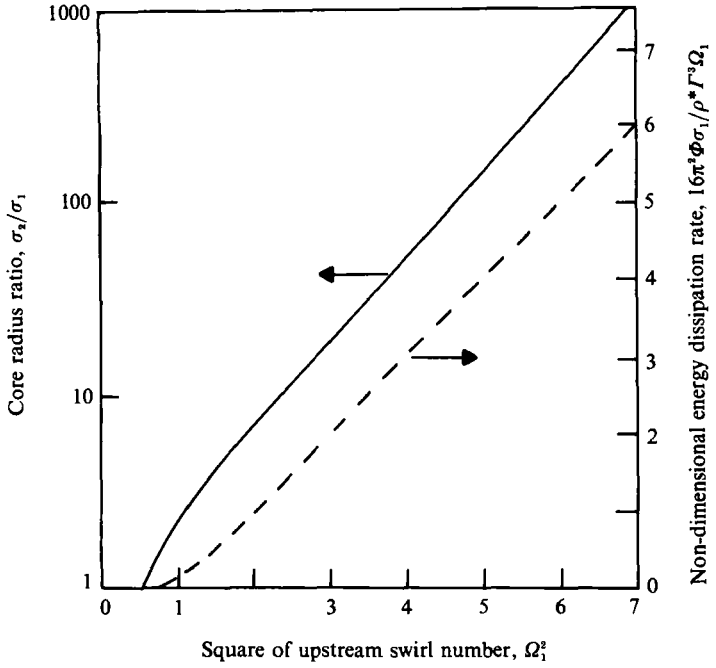

FIGURE 5. Core radius ratio (——) and nondimensional energy dissipation rate (– – –) in stationary axisymmetric vortex breakdowns as a function of the square of the upstream swirl number.

It has been suggested in the literature (Benjamin 1962) that stationary axisymmetric waves may form downstream of an axisymmetric vortex breakdown, although reliable experimental confirmation of this effect still seems to be lacking. Equations (4.5) may be used to find the jump conditions across a stationary axisymmetric breakdown with downstream waves as follows:

$$\Omega_1^2\left[1-\left(\frac{\sigma_1}{\sigma_2}\right)^2\right]-\ln\left(\frac{\sigma_2}{\sigma_1}\right)=\frac{\sigma_1\Omega_1^2}{4}\frac{\sigma_1}{\sigma_2}\left[\frac{\partial^2\sigma_2}{\partial s^2}-\frac{2}{\sigma_2}\left(\frac{\partial\sigma_2}{\partial s}\right)^2\right], \tag{4.10a}$$

$$-\frac{16\pi^2\sigma_1\Phi}{\rho^*\Gamma^3\Omega_1}=\left[1-\left(\frac{\sigma_1}{\sigma_2}\right)^2\right]\left(\left[1+\left(\frac{\sigma_1}{\sigma_2}\right)^2\right]\Omega_1^2-1\right)-\tfrac{1}{2}\Omega_1^2\left(\frac{\sigma_1}{\sigma_2}\right)^4\left(\frac{\partial\sigma_2}{\partial s}\right)^2$$
$$-\frac{\sigma_1}{2}\left(\frac{\sigma_1}{\sigma_2}\right)\Omega_1^2\left[\frac{\partial^2\sigma_2}{\partial s^2}-\frac{2}{\sigma_2}\left(\frac{\partial\sigma_2}{\partial s}\right)^2\right]. \tag{4.10b}$$

The first and second derivatives of σ_2 in (4.10) can be related to various flow constants as shown in §3.3. Sample calculations from (4.10) for the special case in which the point immediately following the discontinuity is a local maximum of the downstream wave field (i.e. $\partial\sigma_2/\partial s=0, \partial^2\sigma_2/\partial s^2<0$) indicate that the effect of downstream waves is to slightly increase both σ_2/σ_1 and $-16\pi^2\sigma_1\Phi/\rho^*\Gamma^3\Omega_1$ over the values given in figure 5.

4.3. *Helical vortex breakdowns*

For helical breakdowns, we assume that σ is uniform on both sides of the discontinuity but admit the possibility that both σ and Γ may be discontinuous across the breakdown point. The upstream vortex circulation is transformed into both circulation of the downstream vortex and rotation of the helix about its axis; thus, discontinuity of Γ at the breakdown point is a necessary consequence of

Kelvin's circulation law. The momentum supply rate F to the discontinuity point is obtained from (4.3) and (2.44) for helical breakdowns as

$$F = \rho^*\left(\frac{\Gamma_1^2}{16\pi\sigma_1^2}+\frac{\Gamma_2^2}{16\pi\sigma_2^2}\right)[\![\sigma^2\lambda_3]\!], \tag{4.11}$$

and the jump conditions (4.2) then become

$$[\![\sigma^2(w-W)]\!] = 0, \tag{4.12a}$$

$$\sigma_1^2(w_1-W)[\![v\lambda_2+w\lambda_3]\!]-\frac{3}{16\pi^2}[\![\Gamma^2\lambda_3]\!]+\left(\frac{\Gamma_1^2}{16\pi^2\sigma_1^2}+\frac{\Gamma_2^2}{16\pi^2\sigma_2^2}\right)[\![\sigma^2\lambda_3]\!] = 0, \tag{4.12b}$$

$$\tfrac{1}{2}\sigma_1^2(w_1-W)\left[\!\!\left[v^2+w^2+\frac{\Gamma^2}{8\pi^2\sigma^2}\right]\!\!\right]-\frac{3}{16\pi^2}[\![w\Gamma^2]\!]+\frac{W}{16\pi^2}\left(\frac{\Gamma_1^2}{\sigma_1^2}+\frac{\Gamma_2^2}{\sigma_2^2}\right)[\![\sigma^2\lambda_3\cdot\boldsymbol{e}_z]\!] = \frac{1}{\pi\rho^*}\Phi. \tag{4.12c}$$

It is convenient to express our solution in terms of the circulation ratio C, the core radius ratio α and the swirl numbers Ω_1, Ω_2, and Ω_s, defined by

$$C = \frac{\Gamma_2}{\Gamma_1}, \quad \alpha = \frac{\sigma_2}{\sigma_1}, \quad \Omega_1 = \frac{2\pi\sigma_1 w_1}{\Gamma_1}, \quad \Omega_2 = \frac{2\pi\sigma_2 w_2}{\Gamma_2}, \quad \Omega_s = \frac{2\pi\sigma_1 W}{\Gamma_1}. \tag{4.13}$$

Using the expressions for λ_2 and λ_3 given in (3.3), the jump conditions (4.12) yield the following results:

$$\Omega_2 = \Omega_s+\frac{1}{\alpha C}(\Omega_1-\Omega_s), \tag{4.14a}$$

$$\frac{2\pi\sigma_2 v_2}{\Gamma_2} = (\gamma D)\,\Omega_2\left[\frac{\alpha(2C^2-\alpha^2)}{4C\Omega_2(\Omega_1-\Omega_s)}-1\right], \tag{4.14b}$$

$$(\gamma D)^2 = -1+\left[\frac{4\alpha^2\Omega_1(\Omega_1-\Omega_s)-(2\alpha^2-C^2)}{4\alpha^2C\Omega_2(\Omega_1-\Omega_s)-\alpha^2(2C^2-\alpha^2)}\right]^2, \tag{4.14c}$$

$$\begin{aligned}-\frac{16\pi^2\sigma_1\Phi}{\rho^*\Gamma_1^3} = -(\Omega_1-\Omega_s)\Bigg\{&\frac{C^2\Omega_2^2}{\alpha^2}\left[\frac{\alpha(2C^2-\alpha^2)}{4C\Omega_2(\Omega_1-\Omega_s)}-1\right]^2(\gamma D)^2+\frac{C^2\Omega_2^2}{\alpha^2}-\Omega_1^2+\frac{C^2-\alpha^2}{2\alpha^2}\Bigg\}\\ &+\frac{3}{2}\left(\frac{\Omega_2 C^3}{\alpha}-\Omega_1\right)-\frac{\Omega_s}{2}\left[\frac{C^2+\alpha^2}{(1+\gamma^2D^2)^{\frac{1}{2}}}-\left(\frac{C^2}{\alpha^2}+1\right)\right].\end{aligned} \tag{4.14d}$$

Typical experimental observations (e.g. Sarpkaya 1971) of helical breakdowns do not exhibit large or even noticeable recirculating 'bubbles' at the transition point, and it may therefore be interesting to examine the case in which no energy is dissipated at the discontinuity point (i.e. $\Phi = 0$). If we further specialize to stationary breakdowns (i.e. $\Omega_s = 0$), the results (4.14) yield

$$\left.\begin{aligned}\Omega_2 = \frac{\Omega_1}{\alpha C}, \quad \frac{2\pi\sigma_2 v_2}{\Gamma_2} &= (\gamma D)\,\Omega_2\left[\frac{\alpha(2C^2-\alpha^2)}{4C\Omega_1\Omega_2}-1\right],\\ [1+(\gamma D)^2]^{\frac{1}{2}} &= \frac{4\alpha^2\Omega_1^2-(2\alpha^2-C^2)}{4\Omega_1^2-\alpha^2(2C^2-\alpha^2)},\\ C^2 = \left(\frac{2\alpha^6+4\alpha^2\Omega_1^2-2\alpha^2}{4\alpha^4-1}\right)&\pm\left(\frac{\alpha^2}{4\alpha^4-1}\right)[16\Omega_1^4-(16\alpha^4+8)\,\Omega_1^2+9\alpha^4]^{\frac{1}{2}}.\end{aligned}\right\} \tag{4.15}$$

For each value of α, there is only a limited range of Ω_1^2 which yields real values of γD and C. The various regions in (α, Ω_1^2)-space in which helical breakdowns are possible

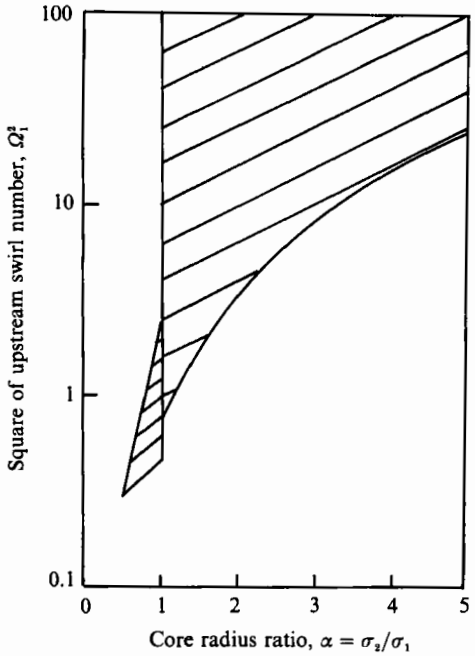

FIGURE 6. Regions in (α, Ω_1^2)-space in which stationary helical vortex breakdown is possible (shaded) and not possible (unshaded) without energy loss at the breakdown point. Notice that the regions $\alpha > 1$ and $\alpha < 1$ are discontinuous.

are shown in figure 6, and we notice considerable differences in these regions for the ranges $\alpha < 1$, $\alpha = 1$ and $\alpha > 1$. For $\alpha = 1$, stationary helical breakdowns are found to be possible only for Ω_1^2 in the range $\frac{3}{4} < \Omega_1^2 < \frac{9}{4}$. For $\frac{1}{2} < \alpha < 1$, distinct upper and lower bounds on Ω_1^2 are found for existence of helical waves, and the limit of the lower bound as $\alpha \to 1^-$ is $\Omega_{1,\min}^2 \to \frac{1}{2}$. No stationary helical breakdown can occur for $\alpha \leqslant \frac{1}{2}$ or for $\Omega_1^2 \leqslant \frac{1}{2}$. For $\alpha > 1$, there is no upper bound on Ω_1^2 for existence of helical waves, and the lower bound increases monotonically with α. Of course, all of the statements apply only for stationary breakdowns with no energy dissipation at the jump, as we have previously prescribed.

The case $\alpha = 1$ is of particular interest both because core radius appears to be nearly continuous across helical breakdowns in many, though not all, experimental situations and because it lies at the transition between two distinct regions in figure 6. Setting $\alpha = 1$ in (4.15) we obtain

$$C^2 = \tfrac{8}{3}\Omega_1^2 - 1, \quad (1+\gamma^2 D^2)^{\frac{1}{2}} = \frac{20\Omega_1^2 - 9}{9 - 4\Omega_1^2}, \quad \Omega_2 = \frac{\Omega_1}{C}, \quad \frac{2\pi\sigma_2 v_2}{\Gamma_2} = (\gamma D)\frac{\Omega_2}{4\Omega_1^2}(\tfrac{4}{3}\Omega_1^2 - 3). \tag{4.16}$$

For all values of Ω_1^2 for which helical breakdowns may occur ($\frac{3}{4} < \Omega_1^2 < \frac{9}{4}$), the sign of v_2 is the same as the sign of γD, assuming positive w.

5. Vortex buckling

In this section, we consider the problem of an initially columnar vortex which spans a length L_0 along the normal between two parallel impermeable plates. The problem is studied in the context of inviscid flow, and so the no-slip condition at the

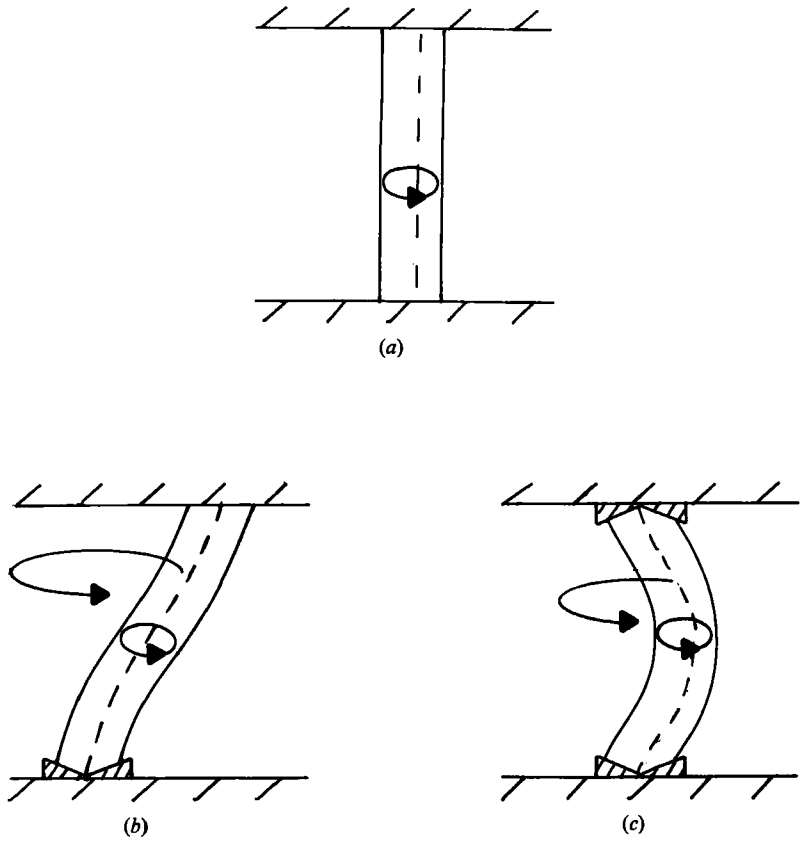

FIGURE 7. Schematic diagram showing unbuckled and buckled shapes of an initially columnar vortex, with closed loops indicating internal circulation of the vortex in the direction of the arrow and open loops indicating circulatory motion of the vortex axis: (*a*) unbuckled shape, (*b*) mode 1 buckled shape with one end fixed, (*c*) mode 2 buckled shape with both ends fixed.

plates is not applied and there is no axial velocity within the vortex. The initially steady vortex is 'compressed' by decreasing the distance between the plates by an amount Δz, and we examine the resulting state of the vortex via a variational theorem of Hamiltonian form constructed from the vortex theory in §2. It is found that if $\Delta z/L_0$ exceeds a critical amount, whose value depends on σ_0/L_0 and on the conditions imposed at the ends, the vortex will bend or 'buckle', whereas if $\Delta z/L_0$ is less than this critical value the vortex will remain columnar. A schematic of the hypothesized buckled vortex shapes and motions is given in figure 7 for the cases in which one end is fixed and the other is free (mode 1) and that in which both ends are fixed (mode 2). The idea of buckling of fluid structures has some precedent in the literature (e.g. Taylor 1968; Cruickshank & Munson 1981), but these studies focus on buckling of highly viscous (non-rotating) jets. The hypothesis of inviscid vortex buckling is treated only theoretically in the present paper; the necessary experimental verification of the phenomenon is still lacking.

5.1. *General variational theorem for inviscid vortices*

A criterion for vortex buckling is derived in the latter part of this section with the use of a general variational theorem for inviscid vortex motion. The variational theorem can be obtained by an extended version of the derivation given by Serrin

(1959, pp. 140–147) for general variational principles in incompressible inviscid flows, to which the reader is referred for a more detailed discussion.

Let us first assume some reference state $\boldsymbol{r} = \boldsymbol{r}(\xi, t)$ and $\boldsymbol{d}_\alpha = \boldsymbol{d}_\alpha(\xi, t)$ for the vortex at time t. We further admit at every point on the vortex a virtual displacement $\delta\boldsymbol{r} = \delta\boldsymbol{r}(\xi, t; \epsilon)$ and a virtual director displacement $\delta\boldsymbol{d}_\alpha = \delta\boldsymbol{d}_\alpha(\xi, t; \epsilon)$, such that the reference state is regained when $\epsilon = 0$. As the parameter ϵ is varied, a family of possible states of the vortex is traced out, and we assume that vortices in this family are continuous and differentiable with respect to spacial and director variables and to ϵ. The membership of this family of vortex states is further restricted to values of $\delta\boldsymbol{r}$ and $\delta\boldsymbol{d}_\alpha$ satisfying mass conservation, the incompressibility constraint, the constraint that the directors remain normal to the vortex axis, and the boundary conditions on the vortex, as well as the requirement of vanishing mechanical power. It is the function of the variational theorem to determine which member or members of this family of states, if any, satisfy the momentum equations (2.9) and (2.10).

The virtual work δU and the virtual change in kinetic energy δK are defined by

$$\delta U = \int_{\xi_1}^{\xi_2} \lambda \boldsymbol{f} \cdot \delta\boldsymbol{r}\, \mathrm{d}\xi + \int_{\xi_1}^{\xi_2} \lambda \boldsymbol{l}^\alpha \cdot \delta\boldsymbol{d}_\alpha\, \mathrm{d}\xi + [\boldsymbol{n} \cdot \delta\boldsymbol{r}]_{\xi_1}^{\xi_2} + [\boldsymbol{m}^\alpha \cdot \delta\boldsymbol{d}_\alpha]_{\xi_1}^{\xi_2}, \tag{5.1}$$

$$\delta K = \delta \int_{\xi_1}^{\xi_2} \tfrac{1}{2}\lambda(\boldsymbol{v} \cdot \boldsymbol{v} + y^{\alpha\beta}\boldsymbol{w}_\alpha \cdot \boldsymbol{w}_\beta)\, \mathrm{d}\xi. \tag{5.2}$$

Taking the scalar products of $\delta\boldsymbol{r}$ and $\delta\boldsymbol{d}_\alpha$ with the ordinary and director momentum equations (2.9) and (2.10), respectively, adding the resulting equations and then integrating over the interval (ξ_1, ξ_2), it can be shown that both a necessary and sufficient condition for any member of the family of vortex states to satisfy the momentum equations is that $\delta\boldsymbol{r}$ and $\delta\boldsymbol{r}_\alpha$ satisfy

$$\frac{\mathrm{d}}{\mathrm{d}t} \int_{\xi_1}^{\xi_2} \lambda(\boldsymbol{v} \cdot \delta\boldsymbol{r} + y^{\alpha\beta}\boldsymbol{w}_\alpha \cdot \delta\boldsymbol{d}_\beta)\, \mathrm{d}\xi - \delta K - \delta U = 0. \tag{5.3}$$

If we further restrict the family of virtual vortex states to those in which both $\delta\boldsymbol{r}$ and $\delta\boldsymbol{d}_\alpha$ vanish everywhere at two times t_0 and t_1, then integration of (5.3) yields Hamilton's principle in the form

$$\delta \int_{t_0}^{t_1} (K + U)\, \mathrm{d}t = 0. \tag{5.4}$$

Equation (5.4) indicates that the integral of $K + U$ from t_0 to t_1 for the 'actual' state is a local extremum or inflexion point of that for neighbouring virtual states, but in fact it is always found in dynamics that the 'actual' state corresponds only to a local minimum of this integral.

5.2. *A criterion for vortex buckling*

In developing a criterion for vortex buckling, we assume the existence of a family of virtual states satisfying the requirements stated in the previous subsection as necessary for satisfaction of Hamilton's equation (5.4). At time t_0, the vortex exists in the initial uncompressed state, and when the vortex is compressed by an amount Δz it adopts one of the family of virtual states, which we call the final state. The differences in $\boldsymbol{r}$ and $\boldsymbol{d}_\alpha$ between the initial state and the actual final state are denoted by $\Delta\boldsymbol{r}$ and $\Delta\boldsymbol{d}_\alpha$, and the differences in $\boldsymbol{r}$ and $\boldsymbol{d}_\alpha$ between the actual final state and other members of the family of virtual states are $\delta\boldsymbol{r}$ and $\delta\boldsymbol{d}_\alpha$. Assuming that $\Delta(K + U)$ is

constant in the final state and letting the time interval (t_1, t_0) be much longer than that required for the vortex to transform from its initial to final state, it follows from (5.4) that $\Delta(K+U)$ achieves a local minimum in the actual final state. The criterion for buckling is obtained by comparing $\Delta(K+U)$ for an unbuckled final state with that for a chosen buckled state, both of which satisfy the momentum equations (2.9)–(2.10), and assuming that buckling occurs whenever

$$\Delta(K+U)_{\text{buckled}} < \Delta(K+U)_{\text{unbuckled}}. \tag{5.5}$$

The approach outlined above parallels classical approaches for buckling of solid rods. The assumption (5.5) can be justified using the Lyapunov instability theorem for continuous systems (Dym 1974). In this approach, a Lyapunov functional V is defined by

$$V = \Delta(K+U)_{\text{buckled}} - \Delta(K+U)_{\text{unbuckled}}. \tag{5.6}$$

From the kinetic energy theorem (2.17) and various other results in §2, we find that for sufficiently slow compression rates, the time derivative of V is given approximately by

$$\dot{V} \approx \int_{\xi_1}^{\xi_2} \frac{\lambda}{\pi\sigma_0^2} \Gamma(\boldsymbol{u}_{\mathrm{B}} \times \boldsymbol{\lambda}_3) \cdot \boldsymbol{v}\, \mathrm{d}\xi. \tag{5.7}$$

Assuming that $u \geqslant 0$ and that $\boldsymbol{u}_{\mathrm{B}}$ has the same form as given by (3.2), we find from (5.7) that $\dot{V} \leqslant 0$. If the condition (5.5) is not satisfied, V and $\dot{V}$ will have opposite signs for all perturbations of the unbuckled state, and it then follows from Lyapunov's stability theorem that the vortex is stable (with respect to some suitably defined metric of the perturbation space). If (5.5) is satisfied, then there will exist some solutions for which V and $\dot{V}$ will have the same sign for arbitrarily small perturbations of the unbuckled state, and for this case it follows from Lyapunov's instability theorem that the vortex is unstable. It should be noted, however, that the approach used in this paper produces only a sufficient, but not necessary, condition for buckling. This shortcoming results from the fact that there is no assurance that the vortex buckles according to the selected buckled state and does not acquire some other buckled state which also satisfies (2.9)–(2.10). In other words, it is possible that multiple modes of buckling may exist (with a given set of boundary conditions), and we do not know that the chosen mode will buckle first.

For the case in which the vortex remains columnar during compression, the core radius σ and change in kinetic energy ΔK after a compression of amount Δz are obtained from the incompressibility requirement $\sigma^2 L = \text{const}$ and (2.8), (2.12), (2.21), (2.24) and (5.2) as

$$\sigma^2 = \sigma_0^2 L_0/(L_0 - \Delta z), \tag{5.8}$$

$$\Delta K = -\frac{\rho^* \Gamma^2 L_0}{16\pi}\left(1 - \frac{\sigma_0^2}{\sigma^2}\right). \tag{5.9}$$

From (5.1) and various of the results in §2, the work ΔU done in going from the initial to the final state is

$$\Delta U = \frac{\rho^* \Gamma^2 L_0}{4\pi}\left[\frac{\sigma_0^2(\sigma - \sigma_0)}{\sigma^3} + \frac{3}{4}\frac{\Delta z}{L}\right], \tag{5.10}$$

where $L = L_0 - \Delta z$ is the compressed vortex length.

In the buckled case, it is assumed that the vortex length L and core radius σ are unchanged during compression, so that $L = L_0$ and $\sigma = \sigma_0$, and the filament

curvature κ is not everywhere zero. We adopt a particularly simple buckled state in which $\tau = u = w = 0, \sigma =$ constant and v and κ are given by

$$v = (\Gamma\kappa/4\pi)[\ln|8/\kappa\sigma| - \tfrac{1}{4}], \quad \kappa = -A\sin(\tfrac{1}{2}n\pi s/L). \tag{5.11}$$

In (5.11), A is a constant, s is measured from the bottom surface and n is defined such that $n = 1$ for mode 1 and $n = 2$ for mode 2 type buckling (see figure 7). The buckled shape (5.11) is found to be an approximate solution of (2.33)–(2.39), which govern the vortex motion, when $\kappa L \ll 1$, and in the remainder of the discussion we will restrict ourselves to this 'small curvature' limit. The compression amount Δz is related to the curvature κ by

$$\Delta z = \frac{1}{2}\int_0^{L_0}\left[\int_0^z \kappa(s)\,\mathrm{d}s\right]^2 \mathrm{d}z. \tag{5.12}$$

Substituting the expression for κ in (5.11) into (5.12) and integrating gives an equation for A as

$$A = \frac{n\pi}{2L}(\Delta z/L)^{\frac{1}{2}}[\tfrac{3}{2} - (2/n\pi)\sin(\tfrac{1}{2}n\pi)]^{-\frac{1}{2}}. \tag{5.13}$$

Also, the radial displacement $r = r(z)$ of the vortex centreline during buckling is given by

$$r = (2L/n\pi)^2 A\sin(\tfrac{1}{2}n\pi z/L). \tag{5.14}$$

The kinetic energy, which is now due not only to the rotation of the vortex but also to the induced bulk motion of the vortex as a whole, is increased from its value in the initial state by an amount

$$\Delta K = \frac{A^2\Gamma^2 L\rho^*\sigma^2}{32\pi}\int_0^1 \sin^2(\tfrac{1}{2}n\pi\eta)\{\tfrac{1}{4} + \ln[\tfrac{1}{8}A\sigma\sin(\tfrac{1}{2}n\pi\eta)]\}^2\,\mathrm{d}\eta. \tag{5.15}$$

From (5.1) and various of the results of §2, the work ΔU exerted on the buckled vortex during compression is

$$\Delta U = \frac{\rho^*\Gamma^2 A^2 L^3}{8\pi^3 n^2} + \frac{3}{16\pi}\rho^*\Gamma^2\Delta z. \tag{5.16}$$

Substituting (5.15), (5.16), (5.9) and (5.10) into (5.5), using (5.13) and again assuming that $\kappa L \ll 1$, the criterion for vortex buckling becomes

$$1 > (2/n\pi)\sin(\tfrac{1}{2}n\pi) + \tfrac{1}{8}\pi^2 n^2(\sigma_0/L_0)^2 I(\sigma_0/L_0, \Delta z/L_0), \tag{5.17}$$

where $I(\sigma_0/L_0, \Delta z/L_0)$ is defined by

$$I\left(\frac{\sigma_0}{L_0}, \frac{\Delta z}{L_0}\right) = \int_0^1 \sin^2(\tfrac{1}{2}n\pi\eta)\left\{\tfrac{1}{4} + \ln\left[\tfrac{1}{8}n\pi\left(\frac{\sigma_0}{L_0}\right)\left(\frac{\Delta z}{L_0}\right)^{\frac{1}{2}}\frac{\sin(\tfrac{1}{2}n\pi\eta)}{(\tfrac{3}{2} - (2/n\pi)\sin(\tfrac{1}{2}n\pi))^{\frac{1}{2}}}\right]\right\}^2 \mathrm{d}\eta. \tag{5.18}$$

For values of σ_0/L_0 and $\Delta z/L_0$ in the range of interest, the integral in (5.18) can be approximated by

$$I \approx \tfrac{1}{2}\ln^2\left\{\tfrac{1}{8}n\pi\frac{\sigma_0}{L_0}(\Delta z/L_0)^{\frac{1}{2}}[\tfrac{3}{2} - (2/n\pi)\sin(\tfrac{1}{2}n\pi)]^{-\frac{1}{2}}\right\}. \tag{5.19}$$

(Comparison of (5.19) with numerical solutions of (5.18) yields an error of less than 5% when the argument of the natural logarithm in (5.19) is less than 0.5.)

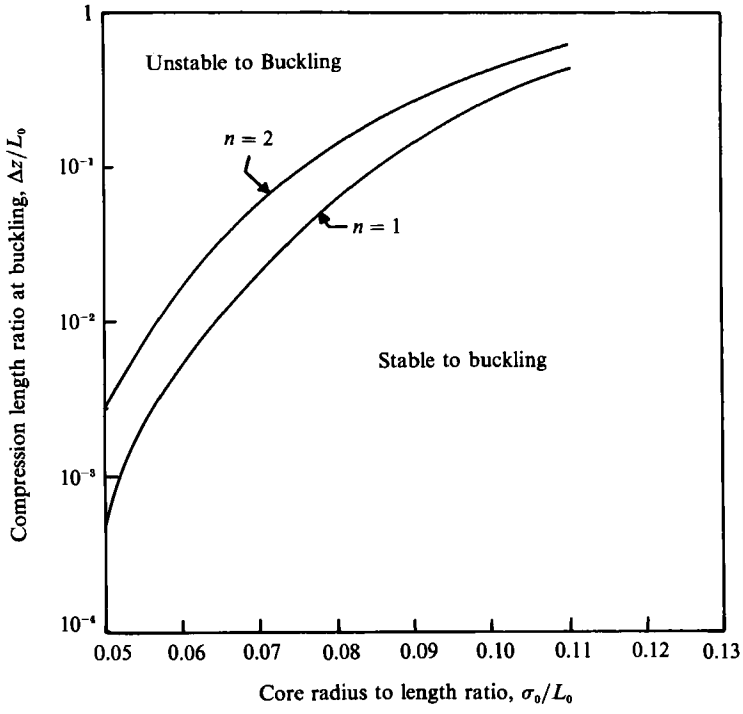

FIGURE 8. Stability regions for vortex buckling as predicted from (5.20).

Substituting (5.19) into (5.17) and solving for $\Delta z/L_0$ gives the compression length for which vortex buckling would occur as

$$\frac{\Delta z}{L_0} \geqslant \left(\frac{8}{n\pi}\right)^2 \left(\frac{L_0}{\sigma_0}\right)^2 \left[\frac{3}{2} - \frac{2}{n\pi}\sin\left(\tfrac{1}{2}n\pi\right)\right] \exp\left\{-\frac{4}{\pi n}\left(\frac{L_0}{\sigma_0}\right)\left[1 - \frac{2}{n\pi}\sin\left(\tfrac{1}{2}n\pi\right)\right]^{\frac{1}{2}}\right\}. \quad (5.20)$$

The predicted value from (5.20) of $\Delta z/L_0$ at buckling is plotted in figure 8 as a function of σ_0/L_0 for both $n = 1$ and $n = 2$. We note from the results in figure 8 that vortex buckling will always occur first in mode 1 ($n = 1$) unless the ends are constrained such that mode 1 is not possible. It is found that a compression Δz of less than 10% of the initial vortex length is sufficient to cause buckling for σ_0/L_0 less than 0.076 (for $n = 2$) or 0.086 (for $n = 1$). The critical compression drops rapidly for smaller values of σ_0/L_0, becoming less than 1% of the initial length for σ_0/L_0 less than 0.057 (for $n = 2$) or 0.064 (for $n = 1$). For σ_0/L_0 greater than 0.095 (for $n = 2$) or 0.102 (for $n = 1$), the compression necessary to produce buckling exceeds the limitations of the linear theory.

It may be useful at this point to briefly summarize the physical processes underlying the vortex buckling phenomenon. As a vortex is compressed, it has the choice of adopting either a buckled or an unbuckled state. In the unbuckled state, work is done on the vortex during compression as the core radius expands and the kinetic energy decreases owing to the shortened vortex length. In the buckled state, the kinetic energy is increased owing to the induced motion of the vortex and work is also done on the vortex as the curvature is increased against the internal constraint force in (2.34). Additionally, some work is done on the vortex at the end points which in the small-compression limit is the same for both buckled and unbuckled states and hence does not contribute to (5.20). From stability considerations, it is found that the

vortex chooses whichever of these states has the smallest value of the change in kinetic energy plus work done. If we were to neglect the increase in kinetic energy due to induced motion of the vortex in the buckled state and the work done by the internal constraint force during bending, we would find that the vortex would buckle for any value of Δz. Alternatively, if we were to neglect the work done by fattening of the unbuckled vortex, we would find that the vortex can never buckle. Considering all of these effects, however, it is found that a discrete non-zero, but finite, buckling point exists such that when the compression $\Delta z/L_0$ is sufficiently small the vortex will remain columnar, but when $\Delta z/L_0$ increases past a critical value, given by (5.20) as a function of σ_0/L_0, the vortex will buckle.

6. Conclusions

The vortex theory developed in §2, as well as the jump conditions in §4.1 and the variational theorem in §5.1, are used in this paper to examine several important problems in vortex dynamics. A number of new results, both mathematical and conceptual, with regard to these problems have been found in the paper, and for clarity these results are briefly summarized in this final section.

One of the major focuses of the paper is to obtain an improved description of nonlinear axisymmetric waves, and a discussion of this problem is given in §3.3. The general theory is used to solve for stationary axisymmetric solitary waves on the core, and it is found that such waves can only exist when the square of the swirl number Ω_0^2 lies between 0.5 and 1. For Ω_0^2 close to 0.5, an asymptotic solution for core radius is found which has the classic sech^2 form, but this solution deviates substantially from the true solution for Ω_0^2 above 0.6. The axisymmetric solitary wave solution obtained here is of particular importance both because of the common observation of such waves in vortex flows (Maxworthy *et al.* 1985) and because a solution for axisymmetric solitary waves cannot be obtained from the theory of LA owing to the neglect of radial inertia.

Jump conditions across axisymmetric and helical vortex breakdowns are derived in §4. The jump conditions for axisymmetric breakdowns between uniform core vortex sections reduce to those of Lundgren & Ashurst (1989). The rate of energy dissipation at the breakdown point is also calculated, and it is found that stationary axisymmetric breakdowns can only occur when the square of the upstream swirl number Ω_1^2 is greater than 0.5. Jump conditions are also given for the case when an axisymmetric downstream wave field exists behind the breakdown point.

The jump condition for helical breakdowns indicate that a stationary helical breakdown can exist with no energy dissipation at the jump for appropriate ranges of Ω_1^2. The core radius may be either continuous or discontinuous across such a jump, but the vortex circulation must be discontinuous. The range of Ω_1^2 in which stationary helical breakdowns can exist depends strongly on the jump in core radius σ across the discontinuity, and in particular, in the common case in which σ is continuous across the breakdown, existence of the breakdown requires that Ω_1^2 fall between $\frac{3}{4}$ and $\frac{9}{4}$. The jump conditions across the breakdown point yield solutions for the jump in vortex circulation across the discontinuity and for the pitch and circumferential velocity of the downstream helical wave.

In §5 it is shown, with use of a form of Hamilton's variational theorem for inviscid vortex motions, that an initially columnar vortex will buckle when it is compressed by an amount $\Delta z/L_0$ which is greater than some critical value. A sufficient criterion for buckling is obtained which allows us to solve for the critical value of $\Delta z/L_0$ as a

function only of the ratio σ_0/L_0 of core radius to vortex length and the boundary conditions at the vortex ends. For values of σ_0/L_0 in the range $0.057 < \sigma_0/L_0 < 0.095$ (with both ends of the vortex fixed) or in the range $0.064 < \sigma_0/L_0 < 0.102$ (with only one end of the vortex fixed), the value of $\Delta z/L_0$ necessary for buckling varies from 0.01 to 0.3. For σ_0/L_0 much below this range extremely small $\Delta z/L_0$ will cause buckling, and for σ_0/L_0 much above this range no buckling will occur within the confines of the linear theory. The major physical processes influencing vortex buckling are discussed at the end of §5.2, but more experimental and theoretical work is needed to come to a complete understanding of this phenomenon.

It is noted in closing that the assumption of circular core cross-section would not be expected to remain valid when the magnitude of the external prescribed flow is comparable in magnitude with the circumferential velocity on the outer edge of the core. The shape of the vortex cross-section is known to sometimes have a strong effect on the vortex behaviour, which is particularly evident in problems involving vortex instability in an external straining flow (Moore & Saffman 1971). We note that the theory of Caulk & Naghdi (1979) for the internal core dynamics is already given for elliptical cross-sections, and extension of the MS derivation of the external forces acting on the vortex involves only the use of straightforward solutions for irrotational flow past rotating elliptical bodies. The method of derivation of the vortex theory in this paper is thus practically the same for circular or elliptical cross-sections, the main difference being that the resulting equations for the elliptical case would be expected to be considerably more complicated than for the circular case.

Appendix. Expansion of inertial forces

A useful expansion of the inertial terms appearing in (2.44) in the terms of the coefficients A_i, B_i and C_i defined in (2.38) is given as follows:

$$\begin{aligned}
&\pi\sigma\frac{\delta}{\delta t}(\sigma\boldsymbol{q})+\pi\sigma\frac{\delta}{\delta t}[\sigma\boldsymbol{u}-\sigma\boldsymbol{\lambda}_3(\boldsymbol{u}\cdot\boldsymbol{\lambda}_3)]\\
&\quad=\pi\sigma[\dot{\sigma}+(u_3-v_3)\,\partial\sigma/\partial s][(2u_1-v_1)\,\boldsymbol{\lambda}_1+(2u_2-v_2)\,\boldsymbol{\lambda}_2]\\
&\qquad+\pi\sigma^2\{[(2\dot{u}_1-\dot{v}_1)+C_1(2u_2-v_2)]\,\boldsymbol{\lambda}_1+[(2\dot{u}_2-\dot{v}_2)+B_2(2u_1-v_1)]\,\boldsymbol{\lambda}_2\\
&\qquad+[B_3(2u_1-v_1)+C_3(2u_2-v_2)]\,\boldsymbol{\lambda}_3\}+\pi\sigma^2(u_3-v_3)\{[\partial/\partial s(2u_1-v_1)\,\boldsymbol{\lambda}_3\\
&\qquad-\tau(2u_2-v_2)\,\boldsymbol{\lambda}_1+[\partial/\partial s(2u_2-v_2)+\tau(2u_1-v_1)]\,\boldsymbol{\lambda}_2-\kappa(2u_1-v_1)\,\boldsymbol{\lambda}_3\},
\end{aligned}\tag{A 1}$$

where $\boldsymbol{u}$ and $\boldsymbol{v}$ are written in terms of their components as

$$\boldsymbol{v}=v_1\boldsymbol{\lambda}_1+v_2\boldsymbol{\lambda}_2+v_3\boldsymbol{\lambda}_3,\quad \boldsymbol{u}=u_1\boldsymbol{\lambda}_1+u_2\boldsymbol{\lambda}_2+u_3\boldsymbol{\lambda}_3.\tag{A 2}$$

REFERENCES

Arms, R. J. & Hama, F. R. 1965 Localized-induction concept on a curved vortex and motion of an elliptic vortex ring. *Phys. Fluids* **8**, 553–559.

Benjamin, T. B. 1962 Theory of the vortex breakdown phenomenon. *J. Fluid Mech.* **14**, 593–629.

Benjamin, T. B. 1967 Some developments in the theory of vortex breakdown. *J. Fluid Mech.* **28**, 65–84.

Betchov, R. 1965 On the curvature and torsion of an isolated vortex filament. *J. Fluid Mech.* **22**, 471–479.

Caulk, D. A. & Naghdi, P. M. 1979 The influence of twist on the motion of straight elliptical jets. *Arch. Rat. Mech. Anal.* **69**, 1–30.

CRUICKSHANK, J. O. & MUNSON, B. R. 1981 Viscous fluid buckling of plane and axisymmetric jets. *J. Fluid Mech.* **113**, 221–239.

DYM, C. L. 1974 *Stability Theory and its Applications to Structural Mechanics*. Noordhoff.

GARG, A. K. & LEIBOVICH, S. 1979 Spectral characteristics of vortex breakdown flowfields. *Phys. Fluids* **22**, 2053–2064.

GREEN, A. E. & NAGHDI, P. M. 1976 Directed fluid sheets. *Proc. R. Soc. Lond.* A **347**, 447–473.

GREEN, A. E., NAGHDI, P. M. & WENNER, M. L. 1974 On the theory of rods. II. Developments by direct approach. *Proc. R. Soc. Lond.* A **337**, 485–507.

KELVIN, LORD 1880 Vibrations of a columnar vortex. *Phil. Mag.* **10**, 155–168.

LUNDGREN, T. S. & ASHURST, W. T. 1989 Area-varying waves on curved vortex tubes with application to vortex breakdown. *J. Fluid Mech.* **200**, 283–307 (referred to herein as LA).

MAXWORTHY, T., HOPFINGER, E. J. & REDEKOPP, L. G. 1985 Wave motions on vortex cores. *J. Fluid Mech.* **151**, 141–165.

MILES, J. & SALMON, R. 1985 Weakly dispersive nonlinear gravity waves. *J. Fluid Mech.* **157**, 519–531.

MOORE, D. W. & SAFFMAN, P. G. 1971 Structure of a line vortex in an imposed strain. In *Aircraft Wake Turbulence and its Detection*, p. 339. Plenum.

MOORE, D. W. & SAFFMAN, P. G. 1972 The motion of a vortex filament with axial flow. *Phil. Trans. R. Soc. Lond.* A **272**, 403–429 (referred to herein as MS).

NAGHDI, P. M. 1980 Finite deformation of elastic rods and shells. *Proc. IUTAM Symp. on Finite Elasticity*, pp. 47–103. Martinus Nijhoff.

SARPKAYA, T. 1971 On stationary and travelling vortex breakdowns. *J. Fluid Mech.* **45**, 545–559.

SERRIN, J. 1959 Mathematical principles of classical fluid mechanics. In *Handbuch der Physik* (ed. S. Flügge), Vol. VIII/1, pp. 125–263. Springer.

TAYLOR, G. I. 1968 Instability of jets, threads and sheets of viscous fluids. *Proc. Intl Congr. Appl. Mech.* Springer.

TRUESDELL, C. & TOUPIN, R. 1960 The classical field theories. In *Handbuch der Physik* (ed. S. Flügge), Vol. III/1, pp. 226–793. Springer.

WEHAUSEN, J. V. & LAITONE, E. V. 1960 Surface waves. In *Handbuch der Physik* (ed. S. Flügge), Vol. IX, pp. 446–778.

WIDNALL, S. E. & BLISS, D. B. 1971 Slender-body analysis of the motion and stability of a vortex filament containing an axial flow. *J. Fluid Mech.* **50**, 335–353 (referred to herein as WB).